the increased intrahepatic vascular resistance in cirrhosis. Furthermore, recent data suggest that sinusoidal remodeling could also be involved in portal hypertension, characterized by the increased density of contractile hepatic stellate cells wrapping around sinusoidal endothelial cells.[2] Previous evidence suggests a pivotal role of sinusoidal vasoconstriction in the pathophysiology of portal hypertension, where hepatic stellate cells operate as contractile machinery in response to vasoconstrictors.[5] Among the various potential vasoconstrictors, we have focused on sphingosine 1-phosphate (S1P), a lipid mediator, which elicits a wide variety of cell responses.[6] Recent investigation has revealed that S1P acts through at least five high-affinity G-protein-coupled receptors referred to as $S1P_{1\text{-}5}$,[7,8] among which $S1P_{1\text{-}3}$ are expressed in hepatic stellate cells.[9] S1P stimulates contractility in rat hepatic stellate cells in culture; the stimulation of contractility is C3 exotoxin-sensitive,[9] and is abrogated by the $S1P_2$ antagonist.[10] Then we observed that S1P enhances portal vein pressure in an *ex vivo* model of isolated perfused rat livers by way of $S1P_2$ with Rho activation.[10] These findings prompted us to examine whether the antagonism of $S1P_2$ could reduce portal vein pressure in an *in vivo* model of portal hypertension.

Materials and Methods

Animals. Male Sprague-Dawley rats were purchased from Japan SLC (Shizuoka, Japan). The conventional $S1P_2$-deficient mice ($S1P_2^{-/-}$ mice) and LacZ-knockin mice at the $S1P_2$ locus ($S1P_2^{LacZ/+}$ mice) were generated as described.[11] Wildtype mice ($S1P_2^{+/+}$ mice) were used as littermate controls. All rats and mice were fed a standard pelleted diet and water *ad libitum* under normal laboratory conditions of 12-hour light/dark cycles.

All animals received humane care and the experimental protocol was approved by Animal Research Committee of the University of Tokyo.

Bile Duct Ligation. The common bile duct was doubly ligated and resected between the two ligation in rats and mice as described.[12]

Hemodynamic Measurement. Rats and mice were anesthetized with sodium pentobarbital (40 mg/kg body weight, intraperitoneally),[13] and polyethylene catheters inserted into the carotid artery and vein of each rat for mean arterial pressure measurement and drug infusion. For mice, drug infusion was performed by way of the tail vein. Portal vein pressure was measured in the portal trunk by way of the ileocolic vein with 24G catheters in rats and mice, which were connected to a polygraph system (AP-601G; Nihon Kohden, Tokyo, Japan). The readings were monitored and saved on a computer using the analog-to-digital PowerLab system (AD Instruments, Colorado Springs, CO). After cannulation of all catheters, animals were stabilized hemodynamically for 5 minutes. Thereafter, mean arterial pressure and portal vein pressure were measured for 30 minutes after the administration of $S1P_2$ antagonist, JTE-013 (Cayman Chemical, Ann Arbor, MI),[14] which was infused intravenously for 1 minute. JTE-013 was dissolved in 10% wellsolve (Celeste, Tokyo, Japan)[15] in saline, and the total infused volume was 0.3 mL in rats. The intravenous infusion of 0.5 mL 10% wellsolve for 1 minute did not affect mean arterial pressure and portal vein pressure in control rats (not shown).

Means of mean arterial pressure and portal vein pressure before the infusion were determined using the measured values for 5 minutes after the hemodynamic stabilization, and those after the administration of $S1P_2$ antagonist were determined using the measured values from 10 minutes to 30 minutes after the infusion.

Immunoblot Analysis. Fresh liver specimens were homogenized in M-PER Mammalian Protein Extraction Reagent (Thermo Fisher Scientific, Rockford, IL) plus Halt Protease Inhibitor Cocktail (Thermo Fisher Scientific). Immunoblot analysis was performed as described,[16] using specific antibodies against Rho kinase (dilution 1:1,000, BD Biosciences Pharmigen, San Diego, CA), moesin (dilution 1:1,000, Santa Cruz Biotechnology, Santa Cruz, CA), phosphorylated moesin (dilution 1:1,000, Santa Cruz Biotechnology), phosphorylated myosin phosphatase targeting subunit 1 (MYPT1 [Thr853]; dilution 1:500, Upstate, Lake Placid, NY), and glyceraldehyde 3-phosphate dehydrogenase (GAPDH; dilution 1:2,000, Santa Cruz Biotechnology). Immunoreactive proteins were visualized using a chemiluminescence kit (GE Healthcare, Little Chalfont, UK), and recorded using a LAS-4000 image analyzer (Fuji Film, Tokyo, Japan).

Quantitative Reverse-Transcription Polymerase Chain Reaction (RT-PCR). Total RNA was isolated from rat and mouse livers using TRizol (Invitrogen) according to the manufacturer's guidelines. One microgram of total RNA was reverse-transcribed with the Transcriptor First Strand cDNA Synthesis kit (Roche Diagnostics, Mannheim, Germany). Real-time PCR for rat S1P receptors was performed using LightCycler 1.5 system (Roche Diagnostics). The reaction was performed in 2 μL cDNA for each analyzed sample using the LightCycler FastStart DNA Master HybProbe Kit (Roche Diagnostics). Primers and Probes were $S1P_1$ (sense: 5′-

GTTTCTGCGGGAAGGAAGTA-3′, antisense: 5′-AGCA AGGAGGCTGAAGACTG-3′ and Universal Probe Library [UPL] probe no. 21; Roche), $S1P_2$ (sense: 5′-CCTGGT CACCGACTCCTG-3′, antisense: 5′-GGCATATGCAAG CCTCTCTC-3′, and UPL probe no. 78), and $S1P_3$ (sense: 5′-ACTTAGCGGTGGCAGCAT-3′, antisense: 5′-GAAAC AGGCTCTCGTTCTGC-3′, and UPL probe no. 26).

Real-time PCR for rat Rho, rat Rho kinase, mouse S1P receptors, and mouse smooth-muscle α-actin was performed using the 7300 Real-Time PCR system (Applied Biosystems, Foster City, CA) and according to the TaqMan method in a 25 μL volume containing 12.5 μL 2 × TaqMan Universal Master Mix, No AmpErase UNG (Applied Biosystems) and 2 μL cDNA. Primers and probes of rat Rho, Rho kinase, and mouse S1P receptors were $S1P_1$ (sense: 5′-TTTA GCCGCAGCAAATCAGA-3′, antisense: 5′-GGTTGT CCCCATCGTCCTT-3′, probe: 5′-AACTCCTCTCA CCCCC-3′), and others as described.[17,18] Mouse smooth-muscle α-actin primers and probe were obtained from Applied Biosystems, TaqMan Gene Expression Assays (Mm00725412_s1). Each target gene expression was normalized with endogenous control gene.

Isolation and Culture of Rat Hepatic Stellate Cells. Hepatic stellate cells were isolated from rats weighing 300 to 400 g as described,[19] with some modification using Optiprep (Axis-Shield PoC AS, Oslo, Norway),[20] and cultured on uncoated plastic tissue-culture dishes (Falcon, Lincoln Park, NJ).

Histological and Immunohistochemical Analyses. Excised liver specimens were fixed immediately in 10% formalin and embedded in paraffin, or were snap-frozen in OCT compound. Serial 4-μm-thick liver tissue sections were deparaffinized and analyzed by hematoxylin-eosin and Sirius Red staining for collagen. Cryosections were fixed and first stained using the β-Galactosidase Staining Kit (Mirus Bio, Madison, WI).[11] Then Sirius Red staining or immunohistochemical analysis for smooth-muscle α-actin was performed using a Vector M.O.M. Immunodetection Kit (Vector Laboratories, Burlingame, CA) in accordance with the protocol specified by the manufacturer, with a ready-to-use mouse monoclonal antibody (PROGEN Biotechnik, Heidelberg, Germany). Sections were counterstained with nuclear fast red.

Measurement of Liver Enzymes. Serum levels of aspartate aminotransferase, alanine aminotransferase, alkaline phosphatase, and gamma-glutamyltransferase were determined using an automated analyzer (Bio Majesty JCA-BM 8040, JEOL, Tokyo, Japan).

Statistical Analyses. Quantitative data are presented as means ± standard error of the mean (SEM). Comparisons between groups were made using Student *t* test. Statistical significance was set at $P < 0.05$.

Table 1. Hemodynamic Parameters at Baseline in Bile Duct-Ligated Rats (BDL) and Sham-Operated Rats (Sham)

Parameters	BDL	Sham	*P* Value
Mean arterial pressure (mm Hg)	95.9 ± 8.7	111.1 ± 3.2	0.18
Portal vein pressure (mm Hg)	9.6 ± 0.7	5.2 ± 0.2	< 0.001

Results are expressed as mean ± SEM (n = 9 for BDL and n = 8 for sham).

Results

Hemodynamic Effects of $S1P_2$ Antagonist on Bile Duct-Ligated Rats. The hemodynamic effects of $S1P_2$ antagonist were examined in rats with bile duct ligation and with sham operation at 4 weeks after the operation. Hemodynamic parameters at baseline in bile duct-ligated rats and sham-operated rats are shown in Table 1. Portal vein pressure was significantly higher in bile duct-ligated rats than in sham-operated rats ($P < 0.001$), and a trend of lower mean arterial pressure in bile duct-ligated rats than in sham-operated rats was noted ($P = 0.18$).

Then, following the intravenous infusion of $S1P_2$ antagonist portal vein pressure was reduced in bile duct-ligated rats, as shown in Fig. 1A; the $S1P_2$ antagonist at 0.1 mg/kg body weight reduced portal vein pressure by 14%, and at 1 mg/kg body weight, by 24%. In contrast, the $S1P_2$ antagonist at 0.1 mg/kg body weight or 1 mg/kg body weight did not alter portal vein pressure in sham-operated rats (Fig. 1A). On the other hand, the $S1P_2$ antagonist at 0.1 mg/kg body weight or 1 mg/kg body weight did not affect mean arterial pressure in bile duct-ligated rats or in sham-operated rats (Fig. 1B). These results indicate that the $S1P_2$ antagonist reduced portal vein pressure without affecting mean arterial pressure only in rats with portal hypertension, but not in control rats.

Effect of $S1P_2$ Antagonist on Rho Kinase Activity in the Livers of Bile Duct-Ligated Rats. Because previous findings revealed that the contraction-mediating vasoconstrictor effector Rho kinase plays a pivotal role in the increase in intrahepatic vascular resistance and vasoconstrictor hyperresponsiveness in portal hypertension,[13,17,21-25] the potential involvement of Rho kinase in lowering the effect of the $S1P_2$ antagonist on portal vein pressure in bile duct-ligated rats at 4 weeks after the operation was examined. As shown in Fig. 2, messenger RNA (mRNA) expressions of Rho and Rho kinase (Fig. 2A) and Rho kinase protein expression (Fig. 2B) in the livers were increased in bile

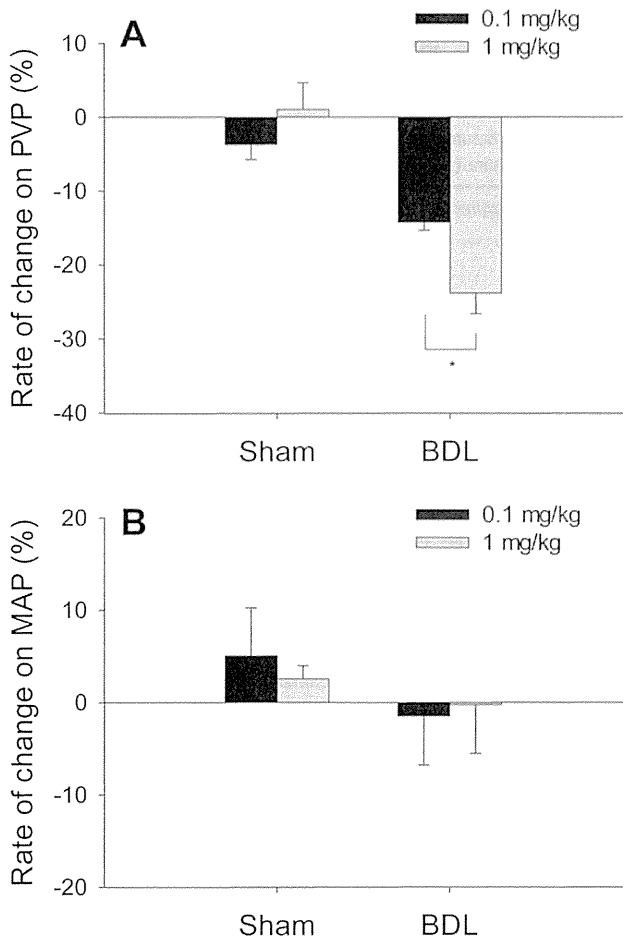

Fig. 1. Hemodynamic effects of $S1P_2$ antagonist on bile duct-ligated rats (BDL) and sham-operated rats (Sham). Portal vein pressure (A) and mean arterial pressure (B) were measured following intravenous infusion of 0.1 or 1 mg/kg body weight $S1P_2$ antagonist. Columns and bars represent means ± SEM of 5 animals. An asterisk indicates a significant difference between rats treated with $S1P_2$ antagonist of 0.1 mg/kg and 1 mg/kg body weight ($P = 0.022$).

duct-ligated rats compared to sham-operated rats, consistent with previous findings.[13,22] Furthermore, Rho kinase activity in the livers was enhanced in bile duct-ligated rats compared to sham-operated rats (Fig. 2C), which is also in line with previous evidence,[13,22] and this enhanced Rho kinase activity in bile duct-ligated livers was reduced after infusion of the $S1P_2$ antagonist, in which Rho kinase activity was analyzed by phosphorylation of moesin and MYPT1 (Thr853), respectively (Fig. 2C,D). Thus, these results suggest that the lowering effect of the $S1P_2$ antagonist on portal vein pressure in rats with portal hypertension is mediated by inhibition of Rho kinase activity.

S1P Receptor mRNA Expression in the Livers of Bile Duct-Ligated Rats and in Cultured Rat Hepatic Stellate Cells. We next examined the potential mechanism of a distinct response to the $S1P_2$ antagonist in portal vein pressure between bile duct-ligated rats and sham-operated rats to examine mRNA expression of S1P receptors, $S1P_1$, $S1P_2$, and $S1P_3$ in the liver. As demonstrated in Fig. 3, $S1P_2$ mRNA expression was increased in the livers of bile duct-ligated rats compared to sham-operated rats at 4 weeks after the operation. Significantly reduced $S1P_1$ mRNA expression, but unaltered $S1P_3$ mRNA expression, in the livers of bile duct-ligated rats was noted. Thus, the increase in $S1P_2$ mRNA expression in the livers of bile duct-ligated rats may explain, at least in part, the distinct responsiveness to $S1P_2$ antagonist in portal vein pressure between bile duct-ligated rats and sham-operated rats.

As described previously, the increased density of contractile hepatic stellate cells could be involved in portal hypertension with liver fibrosis.[2] In the process of liver fibrosis, hepatic stellate cells are known to be activated, and this phenotypic change is also observed in those cells cultured on plastic dishes.[26] Thus, the potential modulation of $S1P_2$ mRNA expression during the process of activation was examined in hepatic stellate cells at 3 and 7 days in culture on plastic dishes; the latter cells were considered more activated than the former cells, although both cells were already activated. As shown in Fig. 3B, $S1P_2$ mRNA expression was significantly increased in hepatic stellate cells at 7 days in culture than that in those cells at 3 days in culture.

S1P Receptor Gene Expressions in the Livers of Bile Duct-Ligated Mice. To identify $S1P_2$-expressing cells in the bile duct-ligated livers, $S1P_2^{LacZ/+}$ mice were employed, in which the LacZ gene is knocked in at the locus of the *S1pr2* allele and LacZ expression is under the control of the endogenous $S1P_2$ promoter.[11] First, we examined the mRNA expression of S1P receptors, $S1P_1$, $S1P_2$, and $S1P_3$ in wildtype mice with bile duct ligation. As demonstrated in Fig. 4, $S1P_2$ mRNA expression was up-regulated in the livers of bile duct-ligated mice at 4 weeks following the operation compared to sham-operated mice, similar to rats, whereas $S1P_1$ and $S1P_3$ mRNA expression was essentially unaltered. Then, $S1P_2$ expression, determined as LacZ activity with 5-bromo-4-chloro-3-indolyl-β-D-galactopyranoside (X-Gal) staining, was evaluated in $S1P_2^{LacZ/+}$ mice with bile duct ligation and sham operation. As depicted in Fig. 5A, $S1P_2$ expression was mainly detected near blood vessels in the liver of sham-operated mice, as previously reported.[11] In contrast, $S1P_2$ expression was highly increased not only near blood vessels but also in other areas in the liver of bile duct-ligated mice (Fig. 5B). The liver tissue

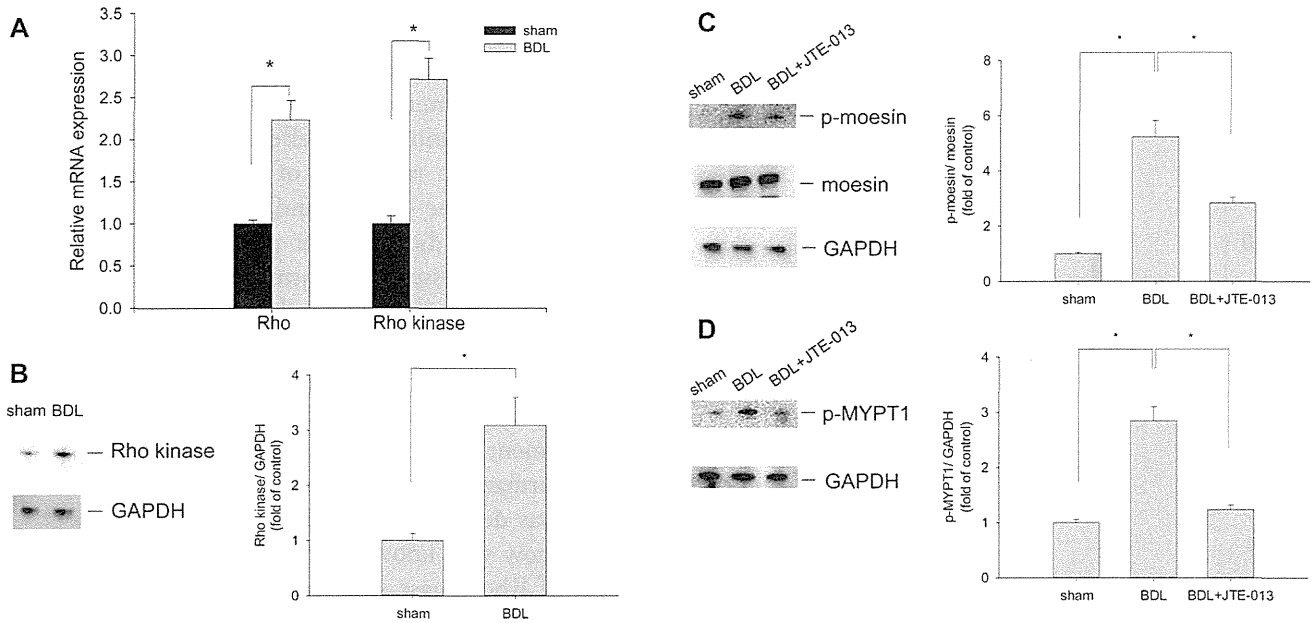

Fig. 2. Effects of $S1P_2$ antagonist on Rho and Rho kinase in the livers of bile duct-ligated rats (BDL). Rho and Rho kinase mRNA (A) and protein (B) expressions were evaluated by quantitative RT-PCR and immunoblot analysis in the livers from bile duct-ligated rats (BDL) compared to sham-operated rats (Sham). Results represent a fold increase of sham-operated rats (means ± SEM, n = 5). mRNAs of Rho ($P = 0.004$) and Rho kinase ($P = 0.001$), and Rho kinase protein ($P = 0.012$) were increased in the livers of bile duct-ligated rats compared to those of sham-operated rats. Rho kinase activity was evaluated by the extent of moesin phosphorylation (C) and MYPT1 phosphorylation (Thr853) (D) in the livers with sham operation, bile duct ligation, and bile duct ligation at 5 minutes following intravenous infusion of 1 mg/kg body weight $S1P_2$ antagonist (BDL+JTE-013). The results represent a fold increase of sham-operated rats (means ± SEM, n = 5). Rho kinase activity was increased with bile duct-ligated livers ($P = 0.001$ in C,D), and this increased activity was reduced by $S1P_2$ antagonist administration ($P = 0.011$ in C and $P = 0.003$ in D). An asterisk indicates a significant difference.

sections from bile duct-ligated mice with X-Gal staining were further submitted to Sirius Red staining to identify collagen fibers, where the vast majority of X-Gal staining was colocalized with fibrosis, found mainly in the periductular area (Fig. 5C) and in lobular septa (Fig. 5D). Finally, smooth-muscle α-actin staining was employed to identify activated hepatic stellate cells. Double staining with antismooth-muscle α-actin and X-Gal staining revealed that the increased X-Gal staining was highly colocalized in smooth-muscle α-actin-expressing cells (Fig. 5E,F).

Rho Kinase Activation and Fibrosis in Liver, and the $S1P_2$ Antagonist Effect on Portal Vein Pressure of $S1P_2^{-/-}$ Mice with Bile Duct Ligation. We evaluated a potential role of S1P and $S1P_2$ in Rho kinase activation in the livers of bile duct-ligated mice using $S1P_2^{-/-}$ mice. Because a time-course analysis revealed that Rho kinase activation was observed as early as 7 days following bile duct ligation in wildtype mice (data not shown), Rho kinase activity was evaluated both in wildtype and $S1P_2^{-/-}$ mice at 7 days following bile duct ligation, in which the increase in Rho kinase activity by bile duct ligation was less in $S1P_2^{-/-}$ mice compared to wildtype mice, as demonstrated in Fig. 6A. These results suggest that S1P and $S1P_2$ contribute, at least in part, to the enhancement of Rho kinase activity in the livers of bile duct-ligated mice.

Then liver fibrosis was evaluated in wildtype and $S1P_2^{-/-}$ mice at 3 weeks following bile duct ligation. Sirius Red staining of the livers showed that fibrosis developed around bile duct and ductal structures and in lobular septa in wildtype mice, whereas less fibrosis was observed predominantly around ductal structures in $S1P_2^{-/-}$ mice (Fig. 6B). Smooth-muscle α-actin mRNA expression in the liver was significantly higher in wildtype mice than in $S1P_2^{-/-}$ mice (Fig. 6C). Collectively, liver fibrosis induced by bile duct ligation was less prominent in $S1P_2^{-/-}$ mice than in wildtype mice.

Next, an intravenous infusion of $S1P_2$ antagonist at 1 mg/kg body weight was performed in wildtype and $S1P_2^{-/-}$ mice at 3 weeks following bile duct ligation. The $S1P_2$ antagonist reduced portal vein pressure in wildtype mice, but not in $S1P_2^{-/-}$ mice (Fig. 6D).

Effect of $S1P_2$ Antagonist on Liver Enzymes and Histology in Control Rats. Because previous studies

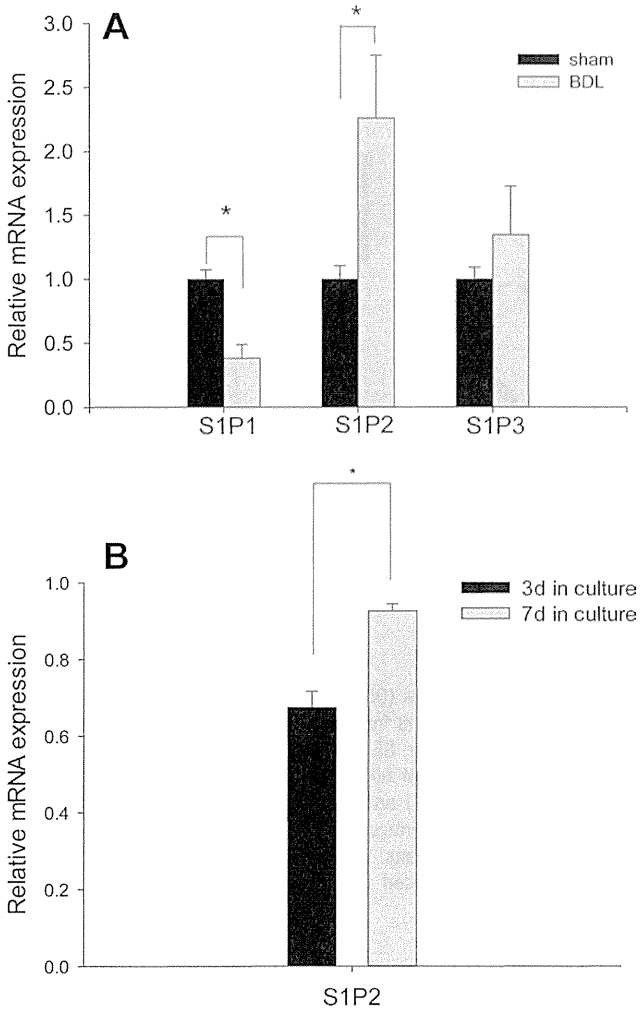

Fig. 3. S1P receptor mRNA expressions in the liver of bile duct-ligated rats and in cultured rat hepatic stellate cells. (A) mRNA expressions of S1P receptors, $S1P_1$, $S1P_2$, and $S1P_3$ were evaluated by quantitative RT-PCR in the livers of sham-operated mice and bile duct-ligated mice at 4 weeks following the operation. Results represent a fold increase of untreated control rats (means ± SEM, n = 7). $S1P_2$ mRNA expression was increased ($P = 0.042$), whereas $S1P_1$ mRNA expression was decreased ($P = 0.0005$) in the livers of bile duct-ligated rats at 4 weeks following the operation. (B) Hepatic stellate cells were isolated from rats and cultured on uncoated plastic dishes. $S1P_2$ mRNA expression was increased in those cells at 7 days in culture than in those at 3 days ($P = 0.015$). Columns and bars represent means ± SEM (n = 3). An asterisk indicates a significant difference.

indicate that $S1P_2$ antagonist exerts its effect also on hepatocytes,[14,27] liver enzymes in serum and liver histology were examined at 24 hours after intravenous injection of the $S1P_2$ antagonist (1 mg/kg body weight) in normal rats to examine whether its intravenous administration might affect hepatocytes. As demonstrated in Fig. 7A-E, serum levels of aspartate aminotransferase, alanine aminotransferase, alkaline phosphatase, and gamma-glutamyltransferase and liver histology were not altered with intravenous injection of the $S1P_2$ antagonist.

Discussion

In the current study, intravenously administered $S1P_2$ antagonist reduced portal vein pressure without affecting mean arterial pressure in cirrhotic rats caused by bile duct ligation. This effect of the $S1P_2$ antagonist involved the reduction of Rho kinase activity in the liver. On the other hand, the same amount of $S1P_2$ antagonist did not alter portal vein pressure and mean arterial pressure in control sham rats. Up-regulation of $S1P_2$ expression was observed in the bile duct-ligated livers of rats and mice, predominantly in hepatic stellate cells as smooth-muscle α-actin-expressing cells. Finally, the contribution of S1P and $S1P_2$ to the enhancement of Rho kinase activity in the liver as well as the formation of liver fibrosis following bile duct ligation was determined in mice.

It is now well known that the intrahepatic up-regulation of Rho kinase signaling plays an important role in the pathophysiology of portal hypertension with increasing hepatic vascular resistance.[22] Thus, Rho kinase has become one of the main targets when establishing the treatment strategy for portal hypertension.[13,17,25,28] On the other hand, among the S1P receptors it has been shown that $S1P_2$ is specifically coupled to Rho and Rho kinase signaling.[29] In fact, we previously showed that S1P increased portal vein pressure by way of $S1P_2$ with the activation of Rho, and presumably of Rho kinase, in isolated perfused rat livers.[10] In the current study, we found that the $S1P_2$

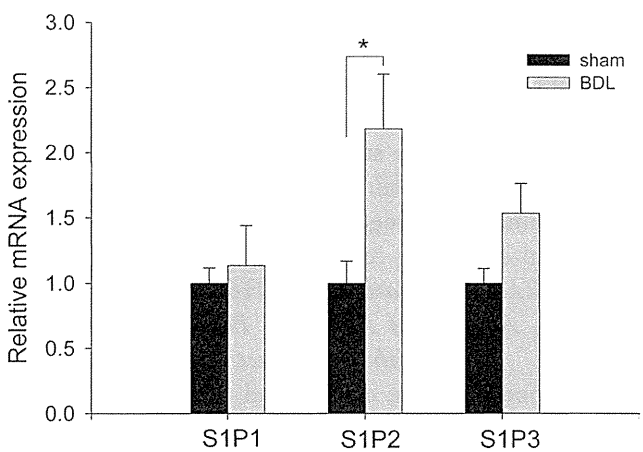

Fig. 4. S1P receptor mRNA expressions in the livers of bile duct-ligated mice. mRNA expressions of S1P receptors, $S1P_1$, $S1P_2$, and $S1P_3$ were evaluated by real-time PCR in the livers of sham-operated mice and bile duct-ligated mice at 4 week following the operation. The results represent a fold of untreated control rats (means ± SEM, n = 8). $S1P_2$ mRNA expression was increased in the livers of bile duct-ligated mice at 4 week following the operation ($P = 0.027$). An asterisk indicates a significant difference from sham-operated mice.

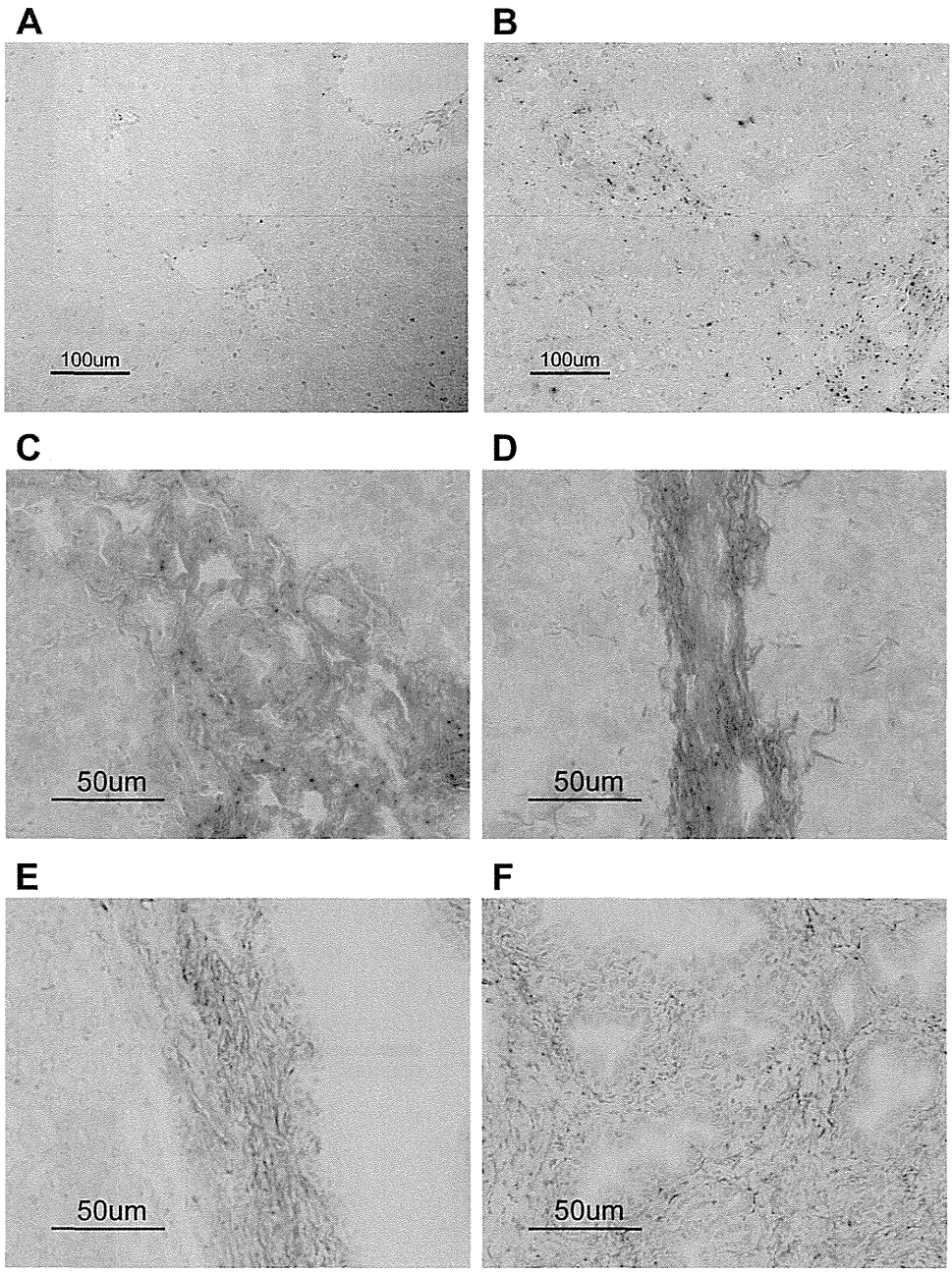

Fig. 5. $S1P_2$ expression in sham-operated $S1P_2^{LacZ/+}$ mice and bile duct-ligated $S1P_2^{LacZ/+}$ mice. $S1P_2$ expression was detected as X-Gal staining in $S1P_2^{LacZ/+}$ mice with sham operation (n = 3) (A) and bile duct ligation at 4 weeks following the operation (n = 6) (B-F). X-Gal stain-positive cells were found near blood vessels in sham-operated mice (A) and those cells were rich in various areas in the liver of bile duct-ligated mice (B). These sections of bile duct-ligated livers were further stained with Sirius Red (C,D), where the vast majority of X-Gal staining was colocalized with fibrosis, found mainly as periductular deposits (C) and as lobular septa (D). Double staining with antismooth- muscle α-actin and X-Gal staining was also performed (E,F), revealing that the increased X-Gal staining was highly colocalized in smooth-muscle α-actin-expressing cells.

antagonist reduced portal vein pressure by inhibiting Rho kinase activity in bile duct-ligated rats.

The effects of various agents on portal hypertension have been examined with acute and chronic administrations.[13,17,22,25,28] When examined with chronic administration, a potential effect on liver fibrosis as well as a direct hemodynamic effect on portal vein pressure should be considered. Indeed, the efficiency of sorafenib in the treatment of portal hypertensive rats may be explained by its antifibrotic effect in the liver.[28,30] Atorvastatin also reportedly lowers portal pressure in cirrhotic rats[17] and attenuates liver fibrosis induced by bile duct ligation in rats.[31] In this context, liver fibrosis was reduced in $S1P_2^{-/-}$ mice with carbon tetrachloride injection[32] and in those with bile duct ligation, suggesting the profibrotic effect of S1P by way of $S1P_2$. Thus, it is likely that chronic administration of $S1P_2$ antagonist may abrogate liver fibrosis, leading to the reduction of portal vein pressure. Other than this, in the current study we evaluated a potential direct effect of the $S1P_2$ antagonist on portal vein pressure with acute intravenous administration.

Of note, the direct inhibition of Rho kinase by intravenously administered fasudil caused a reduction of portal vein pressure and mean arterial pressure in rats with secondary biliary cirrhosis,[13,22] whereas the

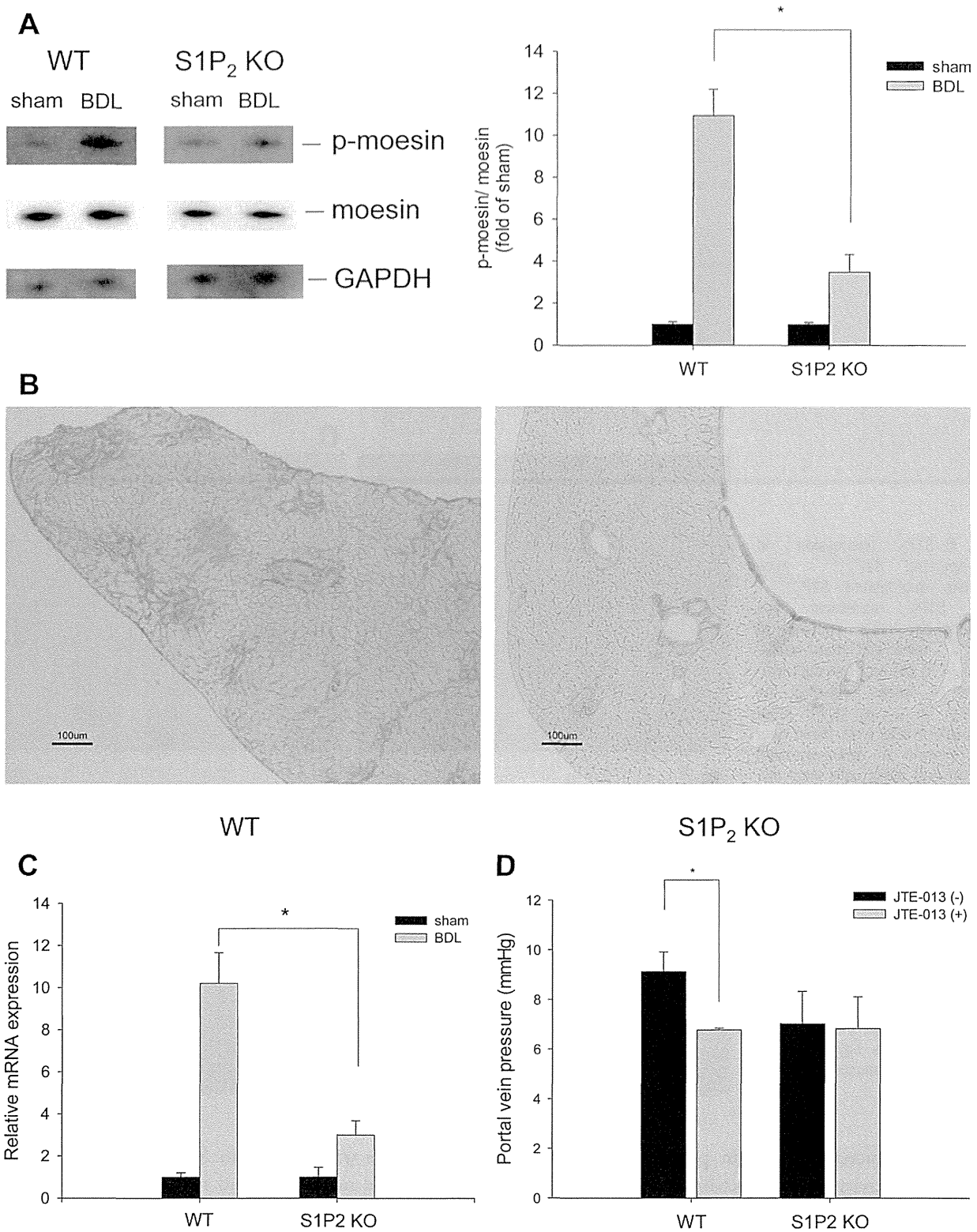

Fig. 6. Rho kinase activity and fibrosis in the livers and $S1P_2$ antagonist effect on portal vein pressure of $S1P_2^{-/-}$ mice following bile duct ligation. (A) Rho kinase activity was determined as phosphorylated moesin in wildtype mice (WT) and $S1P_2^{-/-}$ mice ($S1P_2$ KO) at 7 days following sham operation (sham) or bile duct ligation (BDL). The results represent a fold of sham-operated mice (means ± SEM, $n = 4$). The increase in Rho kinase activity by bile duct ligation was less in $S1P_2^{-/-}$ mice than in wildtype mice ($P = 0.001$). (B) The livers of WT ($n = 5$) and $S1P_2^{-/-}$ mice ($S1P_2$ KO) ($n = 5$) at 3 weeks following bile duct ligation were analyzed by Sirius Red staining. (C) Smooth-muscle α-actin mRNA expression was evaluated by real-time PCR in the livers of WT ($n = 4$) and $S1P_2^{-/-}$ mice ($S1P_2$ KO) ($n = 6$) at 3 weeks following bile duct ligation. The results represent a fold increase of sham-operated mice (means ± SEM, $n = 5$ for wildtype mice and $n = 3$ for $S1P_2^{-/-}$ mice). The increase in smooth-muscle α-actin mRNA expression by bile duct ligation was less in $S1P_2^{-/-}$ mice than in wildtype mice ($P = 0.009$). (D) Portal vein pressure was measured in wildtype mice ($n = 4$) and in $S1P_2^{-/-}$ mice ($n = 3$) before and following intravenous infusion of 1 mg/kg body weight $S1P_2$ antagonist (JTE-013). Columns and bars represent means ± SEM. Portal vein pressure was reduced in wildtype mice ($P = 0.03$), whereas not in $S1P_2^{-/-}$ mice, by $S1P_2$ antagonist administration. An asterisk indicates a significant difference.

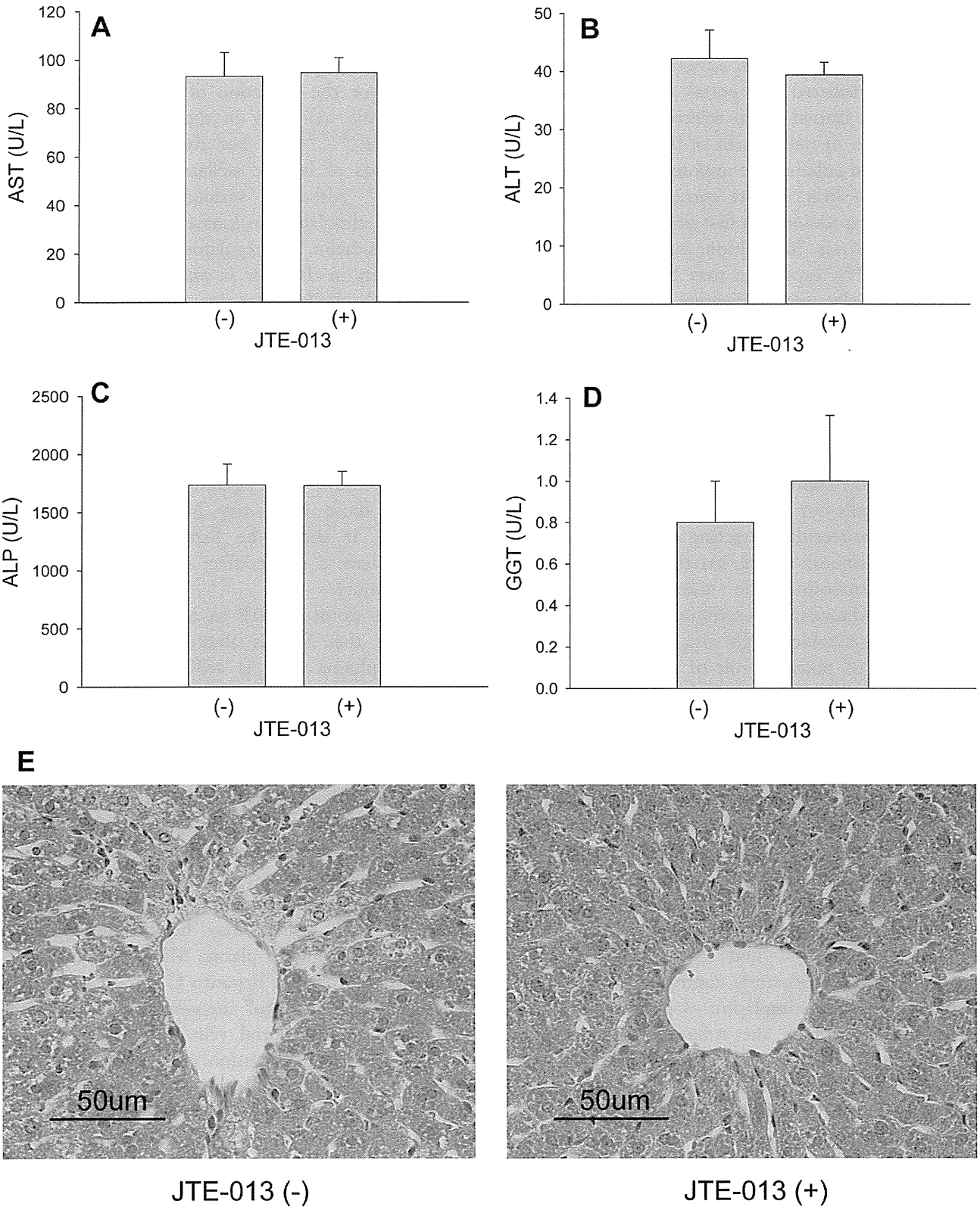

Fig. 7. Effect of $S1P_2$ antagonist on liver enzymes and histology. Serum levels of aspartate aminotransferase (AST) (A), alanine aminotransferase (ALT) (B), alkaline phosphatase (ALP) (C), and gamma-glutamyltransferase (GGT) (D), and liver histology (E) were examined at 24 hours after intravenous injection of $S1P_2$ antagonist (JTE-013; 1 mg/kg body weight) in 6-week-old rats. $S1P_2$ antagonist did not affect serum levels of AST, ALT, ALP, and GGT, and liver histology.

inhibition of Rho kinase by abrogation of the S1P effect through $S1P_2$ led to the reduction only of portal vein pressure, but not of mean arterial pressure in those rats, which may be an advantage when its clinical use is considered for portal hypertension. This finding may be caused by the selective enhancement of $S1P_2$ expression in stellate cells of bile duct-ligated livers, which could enhance the responsiveness to $S1P_2$ antagonist in the liver. In the current study, increased $S1P_2$ mRNA expression was first observed in bile duct-ligated livers in rats. In addition, our evidence suggests that $S1P_2$ mRNA expression may be enhanced in hepatic stellate cells upon activation. To next examine $S1P_2$-expressing cells in the bile duct-ligated livers, we employed $S1P_2^{LacZ/+}$ mice. We confirmed that $S1P_2$ mRNA expression was increased in bile duct-ligated mice similarly to bile duct-ligated rats. $S1P_2$ expression, determined in $S1P_2^{LacZ/+}$ mice, was highly increased in hepatic stellate cells of bile duct-ligated livers. It should be noted that the contribution of not only activated hepatic stellate cells but also portal fibroblasts to liver fibrosis has been recently attracting attention.[33] Because both cells are smooth-muscle α-actin-positive, a certain amount of smooth-muscle α-actin-expressing cells around portal ductular structures in this study could be portal fibroblasts, which might also play a role in portal hypertension.[1] A potential role of portal fibroblasts in the mechanism of reducing portal hypertension by the $S1P_2$ antagonist should be further elucidated. In any case, the selective enhancement of $S1P_2$ expression is assumed in hepatic stellate cells in bile duct-ligated rats to be similar to bile duct-ligated mice, which may explain the selectivity in the reduction of portal vein pressure by the $S1P_2$ antagonist in bile duct-ligated rats.

Although we[32] and others[34] reported a role of $S1P_2$ in the wound-healing response[34] and fibrogenesis[32] upon liver injury, recent evidence demonstrated that $S1P_3$ in rodents,[35,36] and $S1P_1$ and $S1P_3$ in human,[37,38] may importantly contribute to liver fibrosis, focusing on the stimulation of motility of hepatic stellate cells, in which the enhanced expressions of $S1P_1$ and $S1P_3$ but not $S1P_2$ in fibrotic liver were reported. The discrepancy in the evaluation of S1P receptor expressions should be further clarified.

Recent evidence has questioned the selectivity of the S1P receptor agonists or antagonists, including JTE-013, showing that they also affected the responses of other bioactive compounds such as endothelin *in vitro*, according to their concentrations.[39] Although the profile of JTE-013 concentration in plasma after its intravenous administration was not determined in the current study, we assume that the maximum concentration of JTE-013 may be within the range in which JTE-013 selectively acts on the $S1P_2$ receptor, because JTE-013 did not affect portal vein pressure in $S1P_2^{-/-}$ mice with bile duct ligation.

In the liver, the activation of Rho kinase plays an important role, not only in the regulation of portal vein pressure,[13,17,22,25,28] but also in the proliferation and apoptosis of hepatic stellate cells, and hence fibrosis.[16,40,41] Although various agents have been reported to stimulate Rho kinase activity in liver cells, such as endothelin,[42] a regulatory mechanism of Rho kinase activity in the liver *in vivo* has not been elucidated yet. To clarify this point, we employed $S1P_2^{-/-}$ mice and found a smaller activation of Rho kinase caused by bile duct ligation in $S1P_2^{-/-}$ mice compared to in wildtype mice, suggesting that S1P by way of $S1P_2$ plays a pathophysiological role, at least in part, in the regulation of Rho kinase activity upon liver injury. Because $S1P_2^{-/-}$ mice had less fibrosis in the liver after bile duct ligation, reduced Rho kinase activity in those mice may be caused by reduced fibrogenesis. It should be further clarified whether S1P could have a direct effect on Rho kinase in the liver after injury.

A unique point of S1P as a circulating paracrine mediator is that S1P is abundantly present in the blood; its plasma level is ≈300-500 nmol/L.[43] Of note, this level is comparable to the concentration of S1P, readily exerting various effects on cells *in vitro*.[6] Thus, we speculated that the potential modulation of S1P receptor expressions may determine the pathophysiological effects of S1P, a view further supported by the phenotypes of S1P receptor mutants.[44] The current findings of the lowering effect of $S1P_2$ antagonist on portal vein pressure in cirrhotic animals and the reduced activation of Rho kinase in the liver after injury in $S1P_2^{-/-}$ mice may be in line with our hypothesis, although the plasma S1P level was reduced in patients with chronic hepatitis C.[45]

The lowering effect of intravenously administered $S1P_2$ antagonist on portal vein pressure in rats and mice with portal hypertension suggests that the $S1P_2$ antagonist may be useful to urgently reduce portal vein pressure in the clinical setting such as esophageal variceal bleeding, where no effect of the antagonist on arterial pressure could be an advantage. On the other hand, the chronic administration of the $S1P_2$ antagonist could reduce portal vein pressure in cirrhosis patients through a direct hemodynamic effect and further an antifibrotic effect on the liver.[32] Liver fibrosis and portal hypertension may be a good target of the $S1P_2$ antagonist as a therapeutic agent.

References

1. Iwakiri Y, Grisham M, Shah V. Vascular biology and pathobiology of the liver: Report of a single-topic symposium. HEPATOLOGY 2008;47: 1754-1763.
2. Thabut D, Shah V. Intrahepatic angiogenesis and sinusoidal remodeling in chronic liver disease: new targets for the treatment of portal hypertension? J Hepatol 2010;53:976-980.
3. Thalheimer U, Bosch J, Burroughs AK. How to prevent varices from bleeding: shades of grey—the case for nonselective beta blockers. Gastroenterology 2007;133:2029-2036.
4. Speer CA, Ferrentino N. Angiotensin receptor antagonists in portal hypertension: fog over paradise. Gastroenterology 2002;122:1543.
5. Thimgan MS, Yee HF Jr. Quantitation of rat hepatic stellate cell contraction: stellate cells' contribution to sinusoidal resistance. Am J Physiol 1999;277:G137-143.
6. Spiegel S, Merrill AH Jr. Sphingolipid metabolism and cell growth regulation. FASEB J 1996;10:1388-1397.
7. Ishii I, Fukushima N, Ye X, Chun J. Lysophospholipid receptors: signaling and biology. Annu Rev Biochem. 2004;73:321-354.
8. Gardell SE, Dubin AE, Chun J. Emerging medicinal roles for lysophospholipid signaling. Trends Mol Med. 2006;12:65-75.
9. Ikeda H, Yatomi Y, Yanase M, Satoh H, Maekawa H, Ogata I, et al. Biological activities of novel lipid mediator sphingosine 1-phosphate in rat hepatic stellate cells. Am J Physiol Gastrointest Liver Physiol 2000; 279:G304-310.
10. Ikeda H, Nagashima K, Yanase M, Tomiya T, Arai M, Inoue Y, et al. Sphingosine 1-phosphate enhances portal pressure in isolated perfused liver via S1P2 with Rho activation. Biochem Biophys Res Commun. 2004;320:754-759.
11. Du W, Takuwa N, Yoshioka K, Okamoto Y, Gonda K, Sugihara K, et al. S1P(2), the G protein-coupled receptor for sphingosine-1-phosphate, negatively regulates tumor angiogenesis and tumor growth in vivo in mice. Cancer Res 2010;70:772-781.
12. Kountouras J, Billing BH, Scheuer PJ. Prolonged bile duct obstruction: a new experimental model for cirrhosis in the rat. Br J Exp Pathol. 1984;65:305-311.
13. Anegawa G, Kawanaka H, Yoshida D, Konishi K, Yamaguchi S, Kinjo N, et al. Defective endothelial nitric oxide synthase signaling is mediated by rho-kinase activation in rats with secondary biliary cirrhosis. HEPATOLOGY 2008;47:966-977.
14. Ikeda H, Satoh H, Yanase M, Inoue Y, Tomiya T, Arai M, et al. Antiproliferative property of sphingosine 1-phosphate in rat hepatocytes involves activation of Rho via Edg-5. Gastroenterology 2003;124: 459-469.
15. Hamid KA, Lin Y, Gao Y, Katsumi H, Sakane T, Yamamoto A. The effect of wellsolve, a novel solubilizing agent, on the intestinal barrier function and intestinal absorption of griseofulvin in rats. Biol Pharm Bull 2009;32:1898-1905.
16. Ikeda H, Nagashima K, Yanase M, Tomiya T, Arai M, Inoue Y, et al. Involvement of Rho/Rho kinase pathway in regulation of apoptosis in rat hepatic stellate cells. Am J Physiol Gastrointest Liver Physiol 2003; 285:G880-886.
17. Trebicka J, Hennenberg M, Laleman W, Shelest N, Biecker E, Schepke M, et al. Atorvastatin lowers portal pressure in cirrhotic rats by inhibition of RhoA/Rho-kinase and activation of endothelial nitric oxide synthase. HEPATOLOGY 2007;46:242-253.
18. Graler MH, Goetzl EJ. The immunosuppressant FTY720 down-regulates sphingosine 1-phosphate G-protein-coupled receptors. FASEB J 2004;18:551-553.
19. Ikeda H, Fujiwara K. Cyclosporin A and FK-506 in inhibition of rat Ito cell activation in vitro. HEPATOLOGY 1995;21:1161-1166.
20. Valatas V, Xidakis C, Roumpaki H, Kolios G, Kouroumalis EA. Isolation of rat Kupffer cells: a combined methodology for highly purified primary cultures. Cell Biol Int 2003;27:67-73.
21. Hennenberg M, Biecker E, Trebicka J, Jochem K, Zhou Q, Schmidt M, et al. Defective RhoA/Rho-kinase signaling contributes to vascular hypocontractility and vasodilation in cirrhotic rats. Gastroenterology 2006;130:838-854.
22. Zhou Q, Hennenberg M, Trebicka J, Jochem K, Leifeld L, Biecker E, et al. Intrahepatic upregulation of RhoA and Rho-kinase signalling contributes to increased hepatic vascular resistance in rats with secondary biliary cirrhosis. Gut 2006;55:1296-1305.
23. Hennenberg M, Trebicka J, Biecker E, Schepke M, Sauerbruch T, Heller J. Vascular dysfunction in human and rat cirrhosis: role of receptor-desensitizing and calcium-sensitizing proteins. HEPATOLOGY 2007; 45:495-506.
24. Hennenberg M, Trebicka J, Sauerbruch T, Heller J. Mechanisms of extrahepatic vasodilation in portal hypertension. Gut 2008;57: 1300-1314.
25. Trebicka J, Leifeld L, Hennenberg M, Biecker E, Eckhardt A, Fischer N, et al. Hemodynamic effects of urotensin II and its specific receptor antagonist palosuran in cirrhotic rats. HEPATOLOGY 2008;47: 1264-1276.
26. Rockey DC, Boyles JK, Gabbiani G, Friedman SL. Rat hepatic lipocytes express smooth muscle actin upon activation in vivo and in culture. J Submicrosc Cytol Pathol 1992;24:193-203.
27. Studer E, Zhou X, Zhao R, Wang Y, Takabe K, Nagahashi M, et al. Conjugated bile acids activate the sphingosine-1-phosphate receptor 2 in primary rodent hepatocytes. HEPATOLOGY 2012;55:267-276.
28. Hennenberg M, Trebicka J, Stark C, Kohistani AZ, Heller J, Sauerbruch T. Sorafenib targets dysregulated Rho kinase expression and portal hypertension in rats with secondary biliary cirrhosis. Br J Pharmacol 2009;157:258-270.
29. Siehler S, Manning DR. Pathways of transduction engaged by sphingosine 1-phosphate through G protein-coupled receptors. Biochim Biophys Acta 2002;1582:94-99.
30. Hennenberg M, Trebicka J, Kohistani Z, Stark C, Nischalke HD, Kramer B, et al. Hepatic and HSC-specific sorafenib effects in rats with established secondary biliary cirrhosis. Lab Invest 2011;91:241-251.
31. Trebicka J, Hennenberg M, Odenthal M, Shir K, Klein S, Granzow M, et al. Atorvastatin attenuates hepatic fibrosis in rats after bile duct ligation via decreased turnover of hepatic stellate cells. J Hepatol 2010;53: 702-712.
32. Ikeda H, Watanabe N, Ishii I, Shimosawa T, Kume Y, Tomiya T, et al. Sphingosine 1-phosphate regulates regeneration and fibrosis after liver injury via sphingosine 1-phosphate receptor 2. J Lipid Res 2009;50: 556-564.
33. Beaussier M, Wendum D, Schiffer E, Dumont S, Rey C, Lienhart A, et al. Prominent contribution of portal mesenchymal cells to liver fibrosis in ischemic and obstructive cholestatic injuries. Lab Invest 2007;87: 292-303.
34. Serriere-Lanneau V, Teixeira-Clerc F, Li L, Schippers M, de Wries W, Julien B, et al. The sphingosine 1-phosphate receptor S1P2 triggers hepatic wound healing. FASEB J 2007;21:2005-2013.
35. Li C, Jiang X, Yang L, Liu X, Yue S, Li L. Involvement of sphingosine 1-phosphate (SIP)/S1P3 signaling in cholestasis-induced liver fibrosis. Am J Pathol 2009;175:1464-1472.
36. Li C, Kong Y, Wang H, Wang S, Yu H, Liu X, et al. Homing of bone marrow mesenchymal stem cells mediated by sphingosine 1-phosphate contributes to liver fibrosis. J Hepatol 2009;50:1174-1183.
37. Li C, Zheng S, You H, Liu X, Lin M, Yang L, et al. Sphingosine 1-phosphate (S1P)/S1P receptors are involved in human liver fibrosis by action on hepatic myofibroblasts motility. J Hepatol 2011;54: 1205-1213.
38. Liu X, Yue S, Li C, Yang L, You H, Li L. Essential roles of sphingosine 1-phosphate receptor types 1 and 3 in human hepatic stellate cells motility and activation. J Cell Physiol 2011;226:2370-2377.
39. Salomone S, Waeber C. Selectivity and specificity of sphingosine-1-phosphate receptor ligands: caveats and critical thinking in characterizing receptor-mediated effects. Front Pharmacol 2011;2:9.
40. Iwamoto H, Nakamuta M, Tada S, Sugimoto R, Enjoji M, Nawata H. A p160ROCK-specific inhibitor, Y-27632, attenuates rat hepatic stellate cell growth. J Hepatol 2000;32:762-770.

41. Tada S, Iwamoto H, Nakamuta M, Sugimoto R, Enjoji M, Nakashima Y, et al. A selective ROCK inhibitor, Y27632, prevents dimethylnitrosamine-induced hepatic fibrosis in rats. J Hepatol 2001;34:529-536.
42. Tangkijvanich P, Tam SP, Yee HF Jr. Wound-induced migration of rat hepatic stellate cells is modulated by endothelin-1 through rho-kinase-mediated alterations in the acto-myosin cytoskeleton. HEPATOLOGY 2001;33:74-80.
43. Ohkawa R, Nakamura K, Okubo S, Hosogaya S, Ozaki Y, Tozuka M, et al. Plasma sphingosine-1-phosphate measurement in healthy subjects: close correlation with red blood cell parameters. Ann Clin Biochem 2008;45:356-363.
44. Yang AH, Ishii I, Chun J. In vivo roles of lysophospholipid receptors revealed by gene targeting studies in mice. Biochim Biophys Acta 2002;1582:197-203.
45. Ikeda H, Ohkawa R, Watanabe N, Nakamura K, Kume Y, Nakagawa H, et al. Plasma concentration of bioactive lipid mediator sphingosine 1-phosphate is reduced in patients with chronic hepatitis C. Clin Chim Acta 2010;411:765-770.

PLOS ONE

Soluble MICA and a *MICA* Variation as Possible Prognostic Biomarkers for HBV-Induced Hepatocellular Carcinoma

Vinod Kumar[1,2]*, Paulisally Hau Yi Lo[1], Hiromi Sawai[3], Naoya Kato[4], Atsushi Takahashi[2], Zhenzhong Deng[1], Yuji Urabe[1], Hamdi Mbarek[1], Katsushi Tokunaga[3], Yasuhito Tanaka[5], Masaya Sugiyama[6], Masashi Mizokami[6], Ryosuke Muroyama[4], Ryosuke Tateishi[7], Masao Omata[7], Kazuhiko Koike[7], Chizu Tanikawa[1], Naoyuki Kamatani[2], Michiaki Kubo[2], Yusuke Nakamura[1], Koichi Matsuda[1]

1 Laboratory of Molecular Medicine, Human Genome Center, Institute of Medical Science, The University of Tokyo, Tokyo, Japan, **2** Center for Genomic Medicine, The Institute of Physical and Chemical Research (RIKEN), Kanagawa, Japan, **3** Department of Human Genetics, Graduate School of Medicine, The University of Tokyo, Tokyo, Japan, **4** Unit of Disease Control Genome Medicine, The Institute of Medical Science, The University of Tokyo, Tokyo, Japan, **5** Department of Clinical Molecular Informative Medicine, Nagoya City University Graduate School of Medical Sciences, Aichi, Japan, **6** The Research Center for Hepatitis and Immunology, National Center for Global Health and Medicine, Chiba, Japan, **7** Department of Gastroenterology, Graduate School of Medicine, The University of Tokyo, Tokyo, Japan

Abstract

MHC class I polypeptide-related chain A (MICA) molecule is induced in response to viral infection and various types of stress. We recently reported that a single nucleotide polymorphism (SNP) rs2596542 located in the *MICA* promoter region was significantly associated with the risk for hepatitis C virus (HCV)-induced hepatocellular carcinoma (HCC) and also with serum levels of soluble MICA (sMICA). In this study, we focused on the possible involvement of MICA in liver carcinogenesis related to hepatitis B virus (HBV) infection and examined correlation between the *MICA* polymorphism and the serum sMICA levels in HBV-induced HCC patients. The genetic association analysis revealed a nominal association with an SNP rs2596542; a G allele was considered to increase the risk of HBV-induced HCC ($P = 0.029$ with odds ratio of 1.19). We also found a significant elevation of sMICA in HBV-induced HCC cases. Moreover, a G allele of SNP rs2596542 was significantly associated with increased sMICA levels ($P = 0.009$). Interestingly, HCC patients with the high serum level of sMICA (>5 pg/ml) exhibited poorer prognosis than those with the low serum level of sMICA (≤5 pg/ml) ($P = 0.008$). Thus, our results highlight the importance of *MICA* genetic variations and the significance of sMICA as a predictive biomarker for HBV-induced HCC.

Citation: Kumar V, Yi Lo PH, Sawai H, Kato N, Takahashi A, et al. (2012) Soluble MICA and a *MICA* Variation as Possible Prognostic Biomarkers for HBV-Induced Hepatocellular Carcinoma. PLoS ONE 7(9): e44743. doi:10.1371/journal.pone.0044743

Editor: Erica Villa, University of Modena & Reggio Emilia, Italy

Received May 3, 2012; **Accepted** August 7, 2012; **Published** September 14, 2012

Funding: This work was conducted as a part of the BioBank Japan Project that was supported by the Ministry of Education, Culture, Sports, Science and Technology of the Japanese government. The funders had no role in study design, data collection and analysis, decision to publish, or preparation of the manuscript.

Competing Interests: The authors have declared that no competing interests exist.

* E-mail: koichima@ims.u-tokyo.ac.jp

Introduction

Hepatocellular carcinoma (HCC) reveals a very high mortality rate that is ranked the third among all cancers in the world [1]. HCC is known to develop in a multistep process which has been related to various risk factors such as genetic factors, environment toxins, alcohol and drug abuse, autoimmune disorders, elevated hepatic iron levels, obesity, and hepatotropic viral infections [2]. Among them, chronic infection with hepatitis B virus (HBV) is one of the major etiological factors for developing HCC with considerable regional variations ranging from 20% of HCC cases in Japan to 65% in China [3].

Interestingly, clinical outcome after the exposure to HBV considerably varies between individuals. The great majority of individuals infected with HBV spontaneously eliminate the viruses, but a subset of patients show the persistent chronic hepatitis B infection (CHB), and then progresses to liver cirrhosis and HCC through a complex interplay between multiple genetic and environmental factors [4]. In this regard, genome wide association studies (GWAS) using single nucleotide polymorphisms (SNPs) have highlighted the importance of genetic factors in the pathogenesis of various diseases including CHB as well as HBV-induced HCC [5,6,7,8,9,10,11,12,13]. Recently, we identified a genetic variant located at 4.7 kb upstream of the *MHC class I polypeptide-related chain A* (*MICA*) gene to be strongly associated with hepatitis C virus (HCV) -induced HCC development [14].

MICA is highly expressed on viral-infected cells or cancer cells, and acts as ligand for NKG2D to activate antitumor effects of Natural killer (NK) cells and $CD8^+$ T cells [15,16]. Our previous results indicated that a G allele of SNP rs2596542 was significantly associated with the lower cancer risk and the higher level of soluble MICA (sMICA) in the serum of HCV-induced HCC patients, demonstrating the possible role of MICA as a tumor suppressor. However, elevation of serum sMICA was shown to be associated with poor prognosis in various cancer patients [17,18,19,20].

Matrix metalloproteinases (MMPs) can cleave MICA at a transmembrane domain [21] and release sMICA proteins from cells. Since sMICA was shown to inhibit the antitumor effects of NK cells and $CD8^+$ T cells by reduction of their affinity to binding to target cells [22,23], the effect of MICA in cancer cells would be modulated by the expression of MMPs. To elucidate the role of MICA in HBV-induced hepatocellular carcinogenesis, we here report analysis of the *MICA* polymorphism and serum sMICA level in HBV-induced HCC cases.

Materials and Methods

Study participants

The demographic details of study participants are summarized in Table 1. A total of 181 HCC cases, 597 CHB patients, and 4,549 non-HBV controls were obtained from BioBank Japan that was initiated in 2003 with the funding from the Ministry of Education, Culture, Sports, Science and Technology, Japan [24]. In the Biobank Japan Project, DNA and serum of patients with 47 diseases were collected through collaborating network of 66 hospitals throughout Japan. List of participating hospitals is shown in the following website (http://biobankjp.org/plan/member_hospital.html). A total of 226 HCC cases, 102 CHB patients, and 174 healthy controls were additionally obtained from the University of Tokyo. The diagnosis of chronic hepatitis B was conducted on the basis of HBsAg-seropositivity and elevated serum aminotransferase levels for more than six months according to the guideline for diagnosis and treatment of chronic hepatitis (The Japan Society of Hepatology, http://www.jsh.or.jp/medical/gudelines/index.html). Control Japanese DNA samples (n = 934) were obtained from Osaka-Midosuji Rotary Club, Osaka, Japan. All HCC patients were histopathologically diagnosed. Overall survival was defined as the time from blood sampling for sMICA test to the date of death due to HCC. Patients who were alive on the date of last follow-up were censored on that date. All participants provided written informed consent. This research project was approved by the ethics committee of the University of Tokyo and the ethics committee of RIKEN. All clinical assessments and specimen collections were conducted according to Declaration of Helsinki principles.

SNP genotyping

Genotyping platforms used in this study were shown in Table 1. We genotyped 181 HCC cases and 5,483 non-HBV control samples using either Illumina Human Hap610-Quad or Human Hap550v3. The other samples were genotyped at SNP rs2596542 by the Invader assay system (Third Wave Technologies, Madison, WI).

MICA variable number tandem repeat (VNTR) locus genotyping

Genotyping of the *MICA* VNTR locus in 176 HBV-induced HCC samples was performed using the primers reported previously by the method recommended by Applied Biosystems (Foster City, CA) [14]. Briefly, the 5′ end of forward primer was labeled with 6-FAM, and reverse primer was modified with GTGTCTT non-random sequence at the 5′ end to promote Plus A addition. The PCR products were mixed with Hi-Di Formamide and GeneScan-600 LIZ size standard, and separated by GeneScan system on a 3730×l DNA analyzer (Applied Biosystems, Foster City, CA). GeneMapper software (Applied Biosystems, Foster City, CA) was employed to assign the repeat fragment size (Figure S1).

Quantification of soluble MICA

We obtained serum samples of 111 HBV-positive HCC samples, 129 HCV-positive HCC samples, and 60 non-HBV controls from Biobank Japan. Soluble MICA levels were measured by sandwich enzyme-linked immunosorbent assay, as described in the manufacturer's instructions (R&D Systems, Minneapolis, MN).

Statistical analysis

The association between an SNP rs2596542 and HBV-induced HCC was tested by Cochran-Armitage trend test. The Odds ratios were calculated by considering a major allele as a reference. Statistical comparisons between genotypes and sMICA levels were performed by Kruskal-Wallis test (if more than two classes for comparison) or Wilcoxon rank test using R. Overall survival rate of the patients was analyzed by Kaplan-Meier method in combination with log-rank test with SPSS 20 software. The period for the survival analysis was calculated from the date of blood sampling to the recorded date of death or the last follow-up date. Differences with a P value of <0.05 were considered statistically significant.

Results

Association of SNP rs2596542 with HBV-induced HCC

In order to examine the effect of rs2596542 genotypes on the susceptibility to HBV-induced HCC, a total of 407 HCC cases and 5,657 healthy controls were genotyped. The Cochran Armitage trend test of the data revealed a nominal association

Table 1. Demographic details of subjects analyzed.

Subjects	Source	Genotyping platform	Number of Sample	Female (%)	Age (mean+/−sd)
Liver Cancer	BioBank Japan	Illumina Human Hap610-Quad	181	17.9	62.94±9.42
	University of Tokyo	Invader assay	226		
Control	BioBank Japan	Illumina Human Hap550v3	4549	47.95	55.19±12.5
	Osaka**	Illumina Human Hap550v3	934		
	University of Tokyo	Invader assay	174		
Chronic hepatitis B*	BioBank Japan	Invader assay	597	45.66	61.31±12.6
	University of Tokyo	Invader assay	102		

*Chronic hepatitis B patients without liver cirrhosis and liver cancer during enrollment.
**Healthy volunteers from Osaka Midosuji Rotary Club, Osaka, Japan.
doi:10.1371/journal.pone.0044743.t001

between HBV-induced HCC and rs2596542 in which a risk allele G was more frequent among HBV-induced HCC cases than an A allele (P = 0.029, OR = 1.19, 95% CI: 1.02–1.4; Table 2). To further investigate the effect of rs2596542 on the progression from CHB to HBV-induced HCC, we genotyped a total of 699 CHB cases without HCC. Although the progression risk from CHB to HBV-induced HCC was not statistically significant with rs2596542 (P = 0.197 by the Cochran Armitage trend test with an allelic OR = 1.3 (0.94–1.36); Table 2), we found a similar trend of association in which the frequency of a risk-allele G was higher among HBV-induced HCC patients than that of CHB subjects. Since we previously revealed that an A allele was associated with a higher risk of HCV-induced HCC with OR of 1.36 [14], the s2596542 alleles that increased the risk of HCC were opposite in HBV-induced HCC and HCV-induced HCC.

Soluble MICA levels are associated with SNP rs2596542

We subsequently performed measurement of soluble MICA (sMICA) in serum samples using the ELISA method in 176 HBV-positive HCC cases and 60 non-HBV controls. Nearly 30% of the HBV-induced HCC cases revealed the serum sMICA level of >5 pg/ml (defined as high) while the all control individuals except one showed that of ≤5 pg/ml (defined as low) ($P = 4.5 \times 10^{-6}$; Figure 1A). Then, we examined correlation between SNP rs2596542 genotypes and serum sMICA levels in HBV-positive HCC cases. Interestingly, rs2596542 genotypes were significantly associated with serum sMICA levels (P = 0.009; Figure 1B); 39% of individuals with the GG genotype and 20% of those with the AG genotype were classified as high for serum sMICA, but only 11% of those with the AA genotype were classified as high (AA+AG vs GG; P = 0.003) (Figure 1B). These findings were similar with our previous reports in which a G allele was associated with higher serum sMICA levels in HCV-induced HCC patients [14].

Negative association of variable number of tandem repeat (VNTR) with sMICA level

The *MICA* gene harbors a VNTR locus in exon 5 that consists of 4, 5, 6, or 9 repeats of GCT as well as a G nucleotide insertion into a five-repeat allele (referred as A4, A5, A6, A9, and A5.1, respectively). The insertion of G (A5.1) causes a premature translation termination and results in loss of a transmembrane domain, which may produce the shorter form of the MICA protein that is likely be secreted into serum [25]. However, the association of this VNTR locus with serum sMICA level was controversial among studies [14,26,27,28]. Therefore, we examined the association between the VNTR locus and sMICA level in HBV-induced HCC patients, and found no significant association (Figure S1 and S2), concordant with our previous report for HCV-induced HCC patients [14].

Soluble MICA levels are associated with survival of HCC patients

In order to evaluate the prognostic significance of serum sMICA levels in HCC patients, we performed survival analysis of HCC patients. A total of 111 HBV-infected HCC patients and 129 HCV-infected HCC patients were included in this analysis. The mean survival period for HBV- and HCV-infected patients with less than 5 pg/ml of serum sMICA were 67.1 months (95% CI: 61.1–73.1, n = 83), and 58.2 months (95% CI: 51.4–65.0, n = 85), respectively. On the other hand, for patients with more than 5 pg/ml of serum sMICA, the mean survival periods were 47.8 months (95% CI: 34.8–30.9, n = 28) for HBV-induced HCC patients and 59.5 months (95% CI: 51.9–67.1, n = 44) for HCV-induced HCC patients. The Kaplan-Maier analysis and log-rank test indicated that among HBV-induced HCC subjects, the patients in the high serum sMICA group showed a significantly shorter survival than those in the low serum sMICA (P = 0.008; Figure 2). In addition, we performed multi-variate analysis to test whether sMICA is an independent prognostic factor by including age and gender as covariates. The results revealed significant association of sMICA levels with overall survival (P = 0.017) but not with age and gender (Table S1).However, we found no association between the serum sMICA level and the overall survival in the HCV-induced HCC subjects (P = 0.414; Figure S3). Taken together, our findings imply the distinct roles of the *MICA* variation and sMICA between HBV- and HCV-induced hepatocellular carcinogenesis.

Vascular invasion in HBV-related HCC patients is associated with soluble MICA levels

Since sMICA levels were associated with the overall survival of HBV-related HCC patients, we tested whether sMICA levels affect survival through modulating invasive properties of tumors or size of the tumors. We tested the association between sMICA levels and vascular invasion in 35 HBV-related HCC cases, among whom 7 cases were positive and 21 cases were negative for vascular invasion. We found significant association between sMICA levels and vascular invasion (Figure 3; P = 0.014) in which 7 cases with positive vascular invasion showed high levels of sMICA (mean = 54 pg/ml) than 21 cases without vascular invasion (mean = 7.51 pg/ml). However, we found no association between tumor size and sMICA levels (P = 0.56; data not shown). These results suggest that sMICA may reduce the survival of HBV-related HCC patients by affecting the invasive properties of tumors.

Discussion

Several mechanisms such as HBV-genome integration into host chromosomal DNA [29] and effects of viral proteins including HBx [30] are shown to contribute to development and progression of HCC, while the immune cells such as NK and T cells function as key antiviral and antitumor effectors. MICA protein has been

Table 2. Association between HCC and rs2596542.

SNP	Comparison	Chr	Locus	Case MAF	Control MAF	*P**	OR*	95% CI
rs2596542	HCC vs. Healthy control	6	*MICA*	0.294	0.332	0.029	1.19	1.02–1.4
rs2596542	HCC vs. CHB	6	*MICA*	0.294	0.320	0.197	1.13	0.94–1.36

Note: 407 HCC cases, 699 CHB subjects and 5,657 non-HBV controls were used in the analysis.
Chr.,chromosome; MAF, minor allele frequency; OR, odds ratio for minor allele; CI, confidence interval.
*Obtained by Armitage trend test.
doi:10.1371/journal.pone.0044743.t002

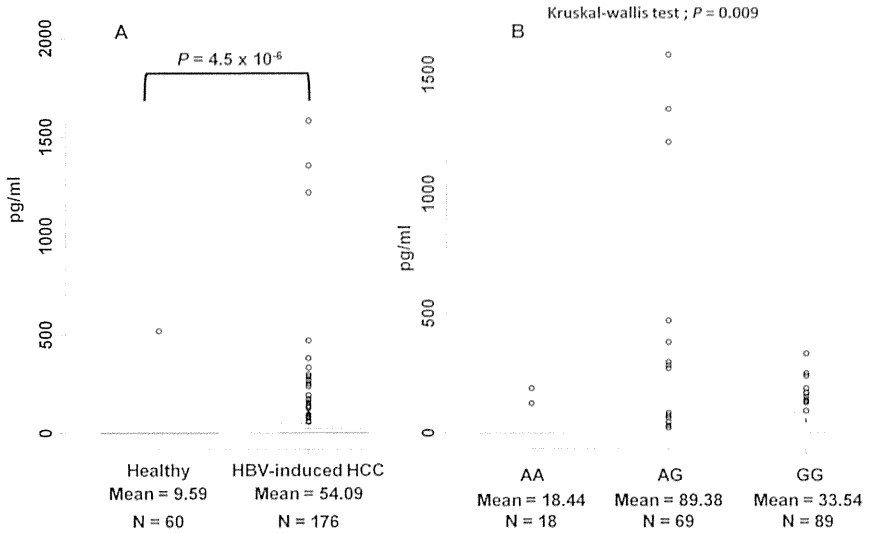

Figure 1. Soluble MICA levels are associated with HBV-related HCC. (A) Correlation between soluble MICA levels and HBV-induced HCC subjects. The y-axis displays the concentration of soluble MICA in pg/ml. The number of independent samples tested in each group is shown in the x-axis. Each group is shown as a box plot and the mean values are shown in the x-axis. The difference between two groups is tested by Wilcoxon rank test. The box plots are plotted using default settings in R. (B) Correlation between soluble MICA levels and rs2596542 genotype in HBV-positive HCC subjects. The x-axis shows the genotypes at rs2596542 and y-axis display the concentration of soluble MICA in pg/ml. Each group is shown as a box plot. $P = 0.027$ and 0.013 for AA vs. GG and AA vs. AG, respectively. The association between genotypes and sMICA levels was tested by Kruskal-wallis test, whereas the difference in the sMICA levels between AA and GG is tested by Wilcoxon rank test. The box plots are plotted using default settings in R.
doi:10.1371/journal.pone.0044743.g001

considered as a stress marker of gastrointestinal epithelial cells because of its induced expression by several external stimuli such as heat, DNA damage, and viral infections [31,32,33,34]. Here, we examined the association of rs2596542 and serum sMICA levels with HBV-induced HCC. Like in HCV-induced HCC [14], our results from ELISA revealed a significantly higher proportion

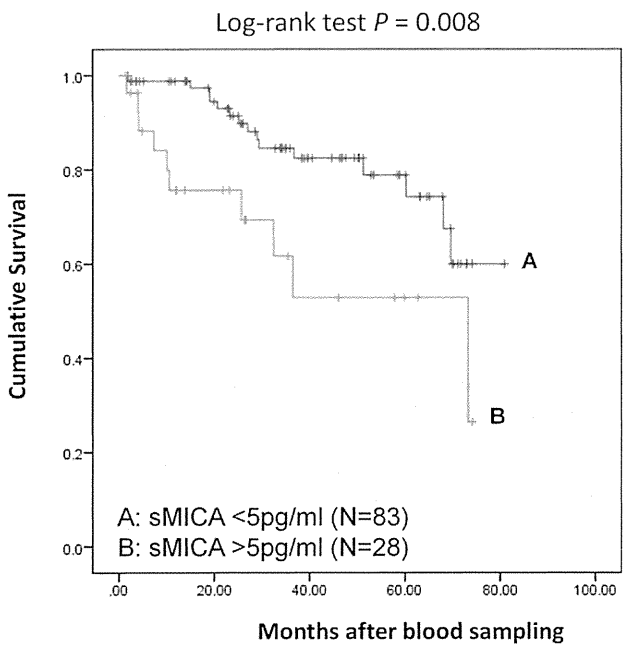

Figure 2. Kaplan-Meier curves of the patients with HBV-induced HCC. The patients were divided into two groups according to their sMICA concentration (high: >5 pg/ml and low: =<5 pg/ml). Statistical difference was analyzed by log-rank test. The y-axis shows the cumulative survival probability and x-axis display the months of the patients survival after blood sampling.
doi:10.1371/journal.pone.0044743.g002

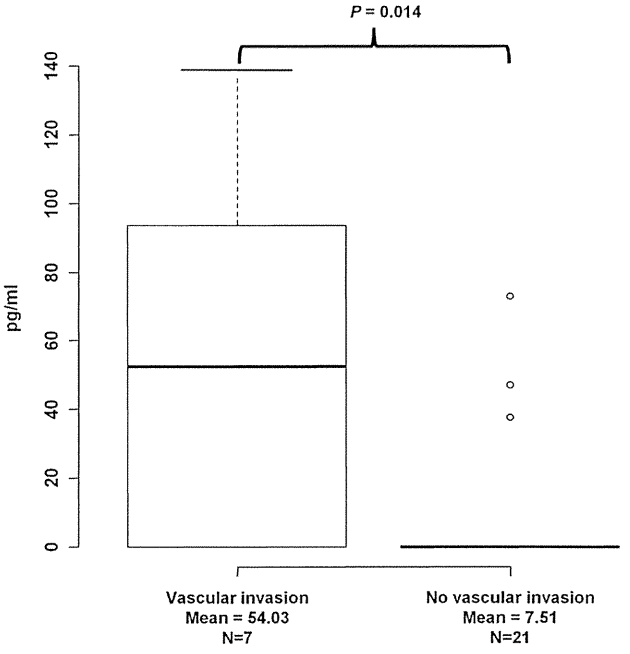

Figure 3. Correlation between soluble MICA levels and vascular invasion in HBV-induced HCC subjects. The y-axis displays the concentration of soluble MICA in pg/ml. The number of independent samples tested in each group is shown in the x-axis. Each group is shown as a box plot and the mean values are shown in the x-axis. The difference between two groups is tested by Wilcoxon rank test. The box plots are plotted using default settings in R.
doi:10.1371/journal.pone.0044743.g003

of high serum sMICA cases (nearly 30%) in the HBV-induced HCC group, compared to non-HBV individuals (1.7%). Moreover, the serum sMICA level was significantly associated with rs2596542, but not with the copy number differences of the VNTR locus, as concordant with our previous report [14].

Several studies have already indicated the roles of sMICA as prognostic markers for different types of malignant diseases [17,18,19,20]. Therefore, it is of medical importance to test whether serum sMICA levels can be used as a prognostic marker for patients with HCC. To our best knowledge, this is the first study to demonstrate the prognostic potential of sMICA for HBV-positive HCC patients; we found 19.3 months of improvement in survival among patients carrying less than 5 pg/ml of serum sMICA, compared to those having more than 5 pg/ml.

On the contrary, we found no significant correlation between sMICA levels and the prognosis of HCV-induced HCC cases. These opposite effects of *MICA* variation could be explained by the following mechanism. The individuals who carry the G allele would express high levels of membrane-bound MICA upon HCV infection and thus lead to the activation of immune cells against virus infected cells. On one hand, HBV infection results in increased expression of membrane-bound MICA as well as MMPs through viral protein HBx [35], which would result in the elevation of sMICA and the reduction of membrane-bound MICA. Since sMICA could block CD8+T cells, NK-CTL, and NK cells, higher sMICA would cause the inactivation of immune surveillance system against HBV infected cells. In other words, HBV may use this strategy to evade immune response and hence, higher levels of sMICA could be associated with lower survival rate among HBV-associated HCC. On the other hand, since HCV is not known to induce the cleavage of membrane bound MICA, individuals with low level membrane bound MICA expression (carriers of rs2596542-allele A) could be inherently susceptible for HCV-induced HCC. Thus, HBx-medicated induction of MMPs could partially explain the intriguing contradictory effect of MICA between HBV-induced HCC and HCV-induced HCC. Since we observed significant correlation of sMICA levels with vascular invasion, it may be the case that high levels of sMICA cause poor prognosis of HBV-related HCC cases by making tumors more aggressive and invasive. However it is important in future to determine the ratio of membrane-bound MICA to sMICA in case of HCV- and HBV-related HCC.

Interestingly, the immune therapy against melanoma patients induced the production of auto-antibodies against MICA [36]. Anti-MICA antibodies would exert antitumor effects through antibody-dependent cellular cytotoxicity against cells expressing membrane-bound MICA and/or activation of NK cells by inhibiting the sMICA-NKG2D interaction. However, further studies are necessary, using well-defined HBV-related HCC cohort, to investigate whether sMICA levels could be included as an additional factor to predict the survival rate among HBV-related HCC subjects. Taken together, our results indicate the potential of *MICA* variant and sMICA as prognostic biomarkers. Thus, MICA could be a useful therapeutic target for HBV-induced HCC.

Supporting Information

Figure S1 MICA repeat genotyping using capillary-based method. The alleles are annotated using GeneMapper software based on the size of the PCR product (185 bp = A4 allele, 188 bp = A5, 189 bp = A5.1, 191 bp = A6 and 200 bp = A9). The inset at the base of each peak shows the size of the PCR product with corresponding allele call by the software. The figure display all observed heterozygotes at A5.1 allele.
(TIF)

Figure S2 MICA VNTR alleles are not associated with soluble MICA levels. Each group is shown as a box plot. The difference in the sMICA values among each group is tested by Wilcoxon rank test. The box plots are plotted using default settings in R.
(TIF)

Figure S3 Kaplan-Meier curves of the patients with HCV-induced HCC. The patients were divided into two groups according to their sMICA concentration (<5 pg/ml or >5 pg/ml). Statistical difference was analyzed by log-rank test. The y-axis shows the cumulative survival probability and x-axis display the months of the patients survival after blood sampling.
(TIF)

Table S1 Clinical parameters of HBV-related HCC patients available for prognostic analyses.
(XLS)

Acknowledgments

We would like to thank all the patients and the members of the Rotary Club of Osaka-Midosuji District 2660 Rotary International in Japan, who donated their DNA for this work. We also thank Ayako Matsui and Hiroe Tagaya (the University of Tokyo), and the technical staff of the Laboratory for Genotyping Development, Center for Genomic Medicine, RIKEN for their technical support.

Author Contributions

Conceived and designed the experiments: VK KM YN. Performed the experiments: VK PHL YU HM ZD. Analyzed the data: VK PHL CT RM. Contributed reagents/materials/analysis tools: YN NK AT MK HS KT YT MS MM RT MO KK NK. Wrote the paper: VK PHL KM YN.

References

1. Kew MC (2010) Epidemiology of chronic hepatitis B virus infection, hepatocellular carcinoma, and hepatitis B virus-induced hepatocellular carcinoma. Pathol Biol (Paris) 58: 273–277.
2. Sherman M (2010) Hepatocellular carcinoma: epidemiology, surveillance, and diagnosis. Semin Liver Dis 30: 3–16.
3. Perz J, Armstrong G, Farrington L, Hutin Y, Bell B (2006) The contributions of hepatitis B virus and hepatitis C virus infections to cirrhosis and primary liver cancer worldwide. J Hepatol 45: 529–538.
4. Chen CJ, Chen DS (2002) Interaction of hepatitis B virus, chemical carcinogen, and genetic susceptibility: multistage hepatocarcinogenesis with multifactorial etiology. Hepatology 36: 1046–1049.
5. Cui R, Okada Y, Jang SG, Ku JL, Park JG, et al. (2011) Common variant in 6q26–q27 is associated with distal colon cancer in an Asian population. Gut 60: 799–805.
6. Kumar V, Matsuo K, Takahashi A, Hosono N, Tsunoda T, et al. (2011) Common variants on 14q32 and 13q12 are associated with DLBCL susceptibility. J Hum Genet England. pp. 436–439.
7. Cui R, Kamatani Y, Takahashi A, Usami M, Hosono N, et al. (2009) Functional variants in ADH1B and ALDH2 coupled with alcohol and smoking synergistically enhance esophageal cancer risk. Gastroenterology 137: 1768–1775.
8. Urabe Y, Tanikawa C, Takahashi A, Okada Y, Morizono T, et al. (2012) A genome-wide association study of nephrolithiasis in the Japanese population identifies novel susceptible loci at 5q35.3, 7p14.3 and 13q14.1. PLOS Genet 8(3): e1002541.
9. Tanikawa C, Urabe Y, Matsuo K, Kubo M, Takahashi A, et al. (2012) A genome-wide association study identifies two susceptibility loci for duodenal ulcer in the Japanese population. Nat Genet 44(4): 430–434.

10. Hata J, Matsuda K, Ninomiya T, Yonemoto K, Matsushita T, et al. (2007) Functional SNP in an Sp1-binding site of AGTRL1 gene is associated with susceptibility to brain infarction. Hum Mol Genet 16: 630–639.
11. Kamatani Y, Wattanapokayakit S, Ochi H, Kawaguchi T, Takahashi A, et al. (2009) A genome-wide association study identifies variants in the HLA-DP locus associated with chronic hepatitis B in Asians. Nat Genet 41: 591–595.
12. Mbarek H, Ochi H, Urabe Y, Kumar V, Kubo M, et al. (2011) A genome-wide association study of chronic hepatitis B identified novel risk locus in a Japanese population. Human Molecular Genetics 20: 3884–3892.
13. Zhang H, Zhai Y, Hu Z, Wu C, Qian J, et al. (2010) Genome-wide association study identifies 1p36.22 as a new susceptibility locus for hepatocellular carcinoma in chronic hepatitis B virus carriers. Nat Genet 42: 755–758.
14. Kumar V, Kato N, Urabe Y, Takahashi A, Muroyama R, et al. (2011) Genome-wide association study identifies a susceptibility locus for HCV-induced hepatocellular carcinoma. Nature genetics 43: 455–458.
15. Jinushi M, Takehara T, Tatsumi T, Kanto T, Groh V, et al. (2003) Expression and role of MICA and MICB in human hepatocellular carcinomas and their regulation by retinoic acid. Int J Cancer 104: 354–361.
16. Bauer S, Groh V, Wu J, Steinle A, Phillips JH, et al. (1999) Activation of NK cells and T cells by NKG2D, a receptor for stress-inducible MICA. Science 285: 727–729.
17. Holdenrieder S, Stieber P, Peterfi A, Nagel D, Steinle A, et al. (2006) Soluble MICA in malignant diseases. Int J Cancer 118: 684–687.
18. Nückel H, Switala M, Sellmann L, Horn PA, Dürig J, et al. (2010) The prognostic significance of soluble NKG2D ligands in B-cell chronic lymphocytic leukemia. Leukemia 24: 1152–1159.
19. Tamaki S, Sanefuzi N, Kawakami M, Aoki K, Imai Y, et al. (2008) Association between soluble MICA levels and disease stage IV oral squamous cell carcinoma in Japanese patients. Hum Immunol 69: 88–93.
20. Li K, Mandai M, Hamanishi J, Matsumura N, Suzuki A, et al. (2009) Clinical significance of the NKG2D ligands, MICA/B and ULBP2 in ovarian cancer: high expression of ULBP2 is an indicator of poor prognosis. Cancer Immunol Immunother 58: 641–652.
21. Salih H, Rammensee H, Steinle A (2002) Cutting edge: down-regulation of MICA on human tumors by proteolytic shedding. J Immunol 169: 4098–4102.
22. Groh V, Wu J, Yee C, Spies T (2002) Tumour-derived soluble MIC ligands impair expression of NKG2D and T-cell activation. Nature 419: 734–738.
23. Jinushi M, Takehara T, Tatsumi T, Hiramatsu N, Sakamori R, et al. (2005) Impairment of natural killer cell and dendritic cell functions by the soluble form of MHC class I-related chain A in advanced human hepatocellular carcinomas. J Hepatol 43: 1013–1020.
24. Nakamura Y (2007) The BioBank Japan Project. Clin Adv Hematol Oncol 5: 696–697.
25. Ota M, Katsuyama Y, Mizuki N, Ando H, Furihata K, et al. (1997) Trinucleotide repeat polymorphism within exon 5 of the MICA gene (MHC class I chain-related gene A): allele frequency data in the nine population groups Japanese, Northern Han, Hui, Uygur, Kazakhstan, Iranian, Saudi Arabian, Greek and Italian. Tissue Antigens 49: 448–454.
26. Tamaki S, Sanefuzi N, Ohgi K, Imai Y, Kawakami M, et al. (2007) An association between the MICA-A5.1 allele and an increased susceptibility to oral squamous cell carcinoma in Japanese patients. J Oral Pathol Med 36: 351–356.
27. Tamaki S, Kawakami M, Yamanaka Y, Shimomura H, Imai Y, et al. (2009) Relationship between soluble MICA and the MICA A5.1 homozygous genotype in patients with oral squamous cell carcinoma. Clin Immunol 130: 331–337.
28. Lü M, Xia B, Ge L, Li Y, Zhao J, et al. (2009) Role of major histocompatibility complex class I-related molecules A*A5.1 allele in ulcerative colitis in Chinese patients. Immunology 128: e230–236.
29. Bonilla Guerrero R, Roberts LR (2005) The role of hepatitis B virus integrations in the pathogenesis of human hepatocellular carcinoma. J Hepatol 42: 760–777.
30. Bouchard MJ, Schneider RJ (2004) The enigmatic X gene of hepatitis B virus. J Virol 78: 12725–12734.
31. Groh V, Bahram S, Bauer S, Herman A, Beauchamp M, et al. (1996) Cell stress-regulated human major histocompatibility complex class I gene expressed in gastrointestinal epithelium. Proc Natl Acad Sci U S A 93: 12445–12450.
32. Groh V, Steinle A, Bauer S, Spies T (1998) Recognition of stress-induced MHC molecules by intestinal epithelial gammadelta T cells. Science 279: 1737–1740.
33. Groh V, Rhinehart R, Randolph-Habecker J, Topp M, Riddell S, et al. (2001) Costimulation of CD8alphabeta T cells by NKG2D via engagement by MIC induced on virus-infected cells. Nat Immunol 2: 255–260.
34. Gasser S, Orsulic S, Brown EJ, Raulet DH (2005) The DNA damage pathway regulates innate immune system ligands of the NKG2D receptor. Nature 436: 1186–1190.
35. Lara-Pezzi E, Gomez-Gaviro MV, Galvez BG, Mira E, Iniguez MA, et al. (2002) The hepatitis B virus X protein promotes tumor cell invasion by inducing membrane-type matrix metalloproteinase-1 and cyclooxygenase-2 expression. J Clin Invest 110: 1831–1838.
36. Jinushi M, Hodi F, Dranoff G (2006) Therapy-induced antibodies to MHC class I chain-related protein A antagonize immune suppression and stimulate antitumor cytotoxicity. Proc Natl Acad Sci U S A 103: 9190–9195.

J Gastroenterol (2012) 47:187–194
DOI 10.1007/s00535-011-0477-8

ORIGINAL ARTICLE—LIVER, PANCREAS, AND BILIARY TRACT

Serum gamma-glutamyltransferase level is associated with serum superoxide dismutase activity and metabolic syndrome in a Japanese population

Hayato Nakagawa · Akihiro Isogawa · Ryosuke Tateishi · Mizuki Tani · Haruhiko Yoshida · Minoru Yamakado · Kazuhiko Koike

Received: 27 June 2011 / Accepted: 16 August 2011 / Published online: 6 October 2011

Abstract
Background Serum gamma-glutamyltransferase level has attracted considerable attention as a predictor of various conditions, such as cardiovascular disease and cancer. Although the mechanism that links the serum gamma-glutamyltransferase level to these diseases is not fully understood, one explanation is that gamma-glutamyltransferase may be closely related to oxidative stress. We conducted a large cross-sectional study to evaluate the relationship between serum gamma-glutamyltransferase and oxidative stress.
Methods We examined anti-oxidative stress activity and accumulation of oxidative stress in serum obtained from 2907 subjects who underwent a complete health check-up. We used serum total superoxide dismutase activity as an index of anti-oxidative stress activity. Superoxide dismutase is one of the most important intracellular and extracellular defense systems against superoxide, but the relationship between serum superoxide dismutase activity and the serum gamma-glutamyltransferase level is unclear.
Results The serum gamma-glutamyltransferase level was negatively correlated with serum superoxide dismutase activity, a correlation that was observed even within the normal range. A subgroup analysis stratified by the amount of alcohol consumed also showed a similar correlation. In contrast, the serum gamma-glutamyltransferase level was positively correlated with serum lipid peroxide level, even in the normal range. Furthermore, an increased serum gamma-glutamyltransferase level was significantly associated with the progression of metabolic syndrome and carotid artery intima-media thickness.
Conclusions The serum gamma-glutamyltransferase level, even in the normal range, was significantly associated with anti-oxidative stress activity, the accumulation of oxidative stress, metabolic syndrome, and atherosclerosis. Measuring the serum gamma-glutamyltransferase level is simple and inexpensive, and this level can be used as a sensitive marker of oxidative stress and metabolic syndrome.

Keywords Gamma-glutamyltransferase · Superoxide dismutase · Lipid peroxide · Metabolic syndrome · Atherosclerosis

Abbreviations

ALT	Alanine aminotransferase
BMI	Body mass index
CuZn-SOD	Copper/zinc-containing superoxide dismutase
DBP	Diastolic blood pressure
GGT	Gamma-glutamyltransferase
GSH	Glutathione
HDL-C	High-density lipoprotein-cholesterol
IMT	Intima-media thickness
ROS	Reactive oxygen species
SBP	Systolic blood pressure
TC	Total cholesterol
T-SOD	Total superoxide dismutase

H. Nakagawa (✉) · R. Tateishi · H. Yoshida · K. Koike
Department of Gastroenterology, University of Tokyo, 7-3-1 Hongo, Bunkyo-ku, Tokyo 113-8655, Japan
e-mail: n-hayato@yf7.so-net.ne.jp

H. Nakagawa · M. Tani · M. Yamakado
Center for Multiphasic Health Testing and Services, Mitsui Memorial Hospital, 1 Kanda-Izumi-cho, Chiyoda-ku, Tokyo 101-8643, Japan

A. Isogawa
Department of Internal Medicine, Mitsui Memorial Hospital, 1 Kanda-Izumi-cho, Chiyoda-ku, Tokyo 101-8643, Japan

Introduction

The serum gamma-glutamyltransferase (GGT) level has been widely used as an indicator of liver disease and alcohol consumption [1]. GGT has attracted considerable attention as a predictor of metabolic syndrome, insulin resistance, cardiovascular disease, stroke, and cancer [2–7]. Furthermore, elevated GGT is associated with higher all-cause mortality [8, 9].

The mechanism that links the serum GGT level to various diseases and mortality is not fully understood. One explanation is that GGT may be closely related to oxidative stress [10–12]. GGT is the enzyme responsible for the extracellular catabolism of glutathione (GSH), the main thiol intracellular antioxidant agent in most cells. Because GGT plays important roles in GSH homeostasis, GGT expression increases as an adaptive response upon exposure to oxidative stress. However, paradoxically, GGT is also directly involved in the generation of reactive oxygen species (ROS) under physiological conditions, particularly in the presence of iron or other transition metals [13]. Thus, the serum GGT level may reflect not only the response to oxidative stress, but also the generation and accumulation of oxidative stress. The serum GGT level has been associated with some oxidative stress markers, such as carotenoids, tocopherols, and lipid peroxide (LPO) [14–16].

Superoxide dismutase (SOD) exists in three isoforms: cytosolic copper/zinc-containing SOD (CuZn-SOD), mitochondrial manganese-containing SOD (Mn-SOD), and extracellular SOD [17, 18]. These enzymes contain redox metals in their catalytic centers and dismutate superoxide radicals to hydrogen peroxide and oxygen. SOD is an endogenous free-radical scavenger and one of the most important intracellular and extracellular defense systems against superoxide, an oxygen-derived free radical that has been implicated in various oxidative cell injuries. The measurement of serum total SOD (T-SOD) activity reflects systemic oxidative stress status, and its level is negatively correlated with atherosclerosis [19]. However, the relationship between serum T-SOD activity and the serum GGT level is unclear.

To evaluate the usefulness of the serum GGT level as an oxidative stress marker, we conducted a large cross-sectional study in 2907 subjects who underwent a complete health check-up. We used serum T-SOD and serum LPO levels as indexes of anti-oxidative stress activity and of the accumulation of oxidative stress, respectively. Additionally, to assess the clinical relevance of the serum GGT level, we investigated the association between the serum GGT level, metabolic syndrome, and carotid atherosclerosis.

Methods

Subjects

Between January 2001 and December 2003, 2907 subjects who had undergone general health screening tests, including carotid ultrasonography, at the Center for Multiphasic Health Testing Services, Mitsui Memorial Hospital, were enrolled. In Japan, regular employee health check-ups are mandated by law. Thus, the majority of these subjects had no major health problem. Blood samples were taken after an overnight fast. Data on hepatitis C core antigen and hepatitis B surface antigen were available in 2877 subjects (98.9%); 23 of these 2877 subjects were positive for hepatitis C and 40 were positive for hepatitis B. Because serum GGT levels did not differ between hepatitis-positive (48.0 ± 45.9 IU/L) and -negative (49.1 ± 57.8 IU/L) subjects, the hepatitis-positive subjects were not excluded.

Serum T-SOD activity was routinely determined with a computerized electron spin resonance spectrometer system (JES-FR30; JEOL, Tokyo, Japan) [19]. Serum LPO level was measured using the fluorimetric assay method of Yagi [20]. Carotid artery status was examined using a high-resolution B-mode ultrasonography instrument (Sonolayer SSA270A; Toshiba, Tokyo, Japan), equipped with a 7.5-MHz transducer (PLF-703ST; Toshiba). The carotid arteries were examined bilaterally at the level of the common carotid, the bifurcation, and the internal carotid arteries from transverse and longitudinal orientations. Carotid artery intima-media thickness (IMT) was measured, using a computer-assisted method, by experienced sonographers who were unaware of the subjects' clinical and laboratory findings.

Of the 2907 subjects, 2249 (77.3%) had undergone abdominal ultrasonography. All abdominal ultrasonography was performed with an SSD-5500 system (Aloka, Wallingford, CT, USA) and a 3.5-MHz convex probe. Fatty liver was diagnosed based on a bright liver with hepatorenal echo contrast.

This study was conducted after written informed consent was received from all subjects. The study protocol conformed to the ethical guidelines of the 1975 Declaration of Helsinki and was approved by the ethics committee of Mitsui Memorial Hospital (MEC2009-30).

Analysis

Body mass index (BMI) was calculated as the square of weight (in kg) divided by height (in meters). We defined obesity as BMI ≥ 25 kg/m^2, hypertension as systolic blood pressure $\geq$130 mmHg or diastolic blood pressure

≥85 mmHg, hypertriglyceridemia as a serum triglyceride concentration of ≥150 mg/dL, low high-density lipoprotein-cholesterol (HDL-C) as HDL-C ≤40 mg/dL for men or ≤50 mg/dL for women, and hyperglycemia as a fasting blood sugar level of ≥110 mg/dL. We defined the metabolic syndrome score as the number of these metabolic syndrome markers, based on the National Cholesterol Education Program Adult Treatment Program III definition.

Serum GGT levels were classified in sextiles; cut-off points of the sextiles for serum GGT were 16, 22, 31, 45, and 77 IU/L. We described the six categories defined by these cut-off points as categories A (serum GGT level ≤16 IU/L), B (17–22 IU/L), C (23–31 IU/L), D (32–45 IU/L), E (46–77 IU/L), and F (> 77 IU/L), respectively. We used sextile classification because we reasoned that the highest GGT group should consist of only the subjects with a serum GGT level above the upper normal limit at our institute (74 IU/L). In quartile and quintile classifications, the highest cut-off point of GGT did not exceed the upper normal limit (58 and 65 IU/L, respectively).

Statistical analyses

Data are expressed as means ± standard deviations. Correlations between variables were analyzed using Spearman's rank correlation coefficient. Stepwise multiple linear regression analysis was used to identify variables that were independently related to serum T-SOD activity. Trends in serum T-SOD activity, LPO level, metabolic score, and IMT in relation to serum GGT levels were assessed with the Jonckheere-Terpstra test. Continuous variables were compared with the unpaired Student's *t*-test (parametric) or the Mann–Whitney *U*-test (nonparametric). A *P* value of <0.05 on a two-tailed test was considered statistically significant. Data processing and analyses were performed using StatView (ver. 5.0; SAS Institute, Cary, NC, USA) and SPSS (ver. 14.0; SPSS, Chicago, IL, USA) software.

Results

Subjects' characteristics

The subjects' characteristic are shown in Table 1. The frequencies of hyperglycemia, hypertension, hypertriglyceridemia, low-HDL-cholesterolemia, and obesity were 14.0, 38.1, 26.0, 8.1, and 27.3%, respectively.

Correlation between serum T-SOD activity and GGT level

To assess whether serum T-SOD activity was linked to metabolic syndrome, we investigated the correlations between serum T-SOD activity and clinical parameters associated with metabolic syndrome. Our results revealed significant correlations between serum T-SOD activity and various clinical parameters that tended to decline with the progression of metabolic syndrome, although these correlations were generally weak (Table 2). Of these parameters, serum GGT was most strongly correlated with serum T-SOD activity ($\rho = -0.16$, $P < 0.0001$). To identify variables that were independently related to serum T-SOD activity, we performed multiple linear regression analysis. Serum T-SOD activity could be predicted by serum GGT, HDL-C, alanine aminotransferase (ALT), age, fasting

Table 1 Baseline characteristics

Variables	$n = 2907$
Age (years)	55.2 ± 10.8
Sex (male/female)	1896/1017
BMI (kg/m^2)	23.3 ± 3.1
SBP (mmHg)	124.4 ± 19.2
DBP (mmHg)	77.7 ± 11.7
TC (mg/dL)	209 ± 34.6
HDL-C (mg/dL)	62.1 ± 16.4
TG (mg/dL)	128 ± 115.2
Glucose (mg/dL)	98.9 ± 21.3
Insulin (IU/L)	6.1 ± 3.8
GGT (IU/L)	49.2 ± 57.6
ALT (IU/L)	27.0 ± 31.1
T-SOD (U/ml)	2.9 ± 1.2
LPO (nmol/ml)	0.8 ± 0.9

BMI Body mass index, *SBP* systolic blood pressure, *DBP* diastolic blood pressure, *TC* total cholesterol, *HDL-C* high-density lipoprotein-cholesterol, *TG* triglycerides, *GGT* gamma-glutamyltransferase, *ALT* alanine aminotransferase, *T-SOD* total superoxide dismutase, *LPO* lipid peroxide

Table 2 Correlations between serum T-SOD activity and other parameters

Variables	Spearman's rho	*P*
Age	0.086	<0.0001
BMI	−0.15	<0.0001
SBP	−0.086	<0.0001
DBP	−0.094	<0.0001
TC	0.06	0.011
HDL-C	0.146	<0.0001
TG	−0.129	<0.0001
Glucose	−0.136	<0.0001
Insulin	−0.125	<0.0001
GGT	−0.16	<0.0001
ALT	−0.071	0.0001